Central exclusive production at CMS: recent results and future prospects with the CT-PPS

M.M. Obertino

Università di Torino, INFN Torino

on behalf of the CMS and TOTEM collaborations

EDS Blois 2015 : the 16th conference on Elastic and Diffractive scattering

Borgo, Corsica, 2 July 2015

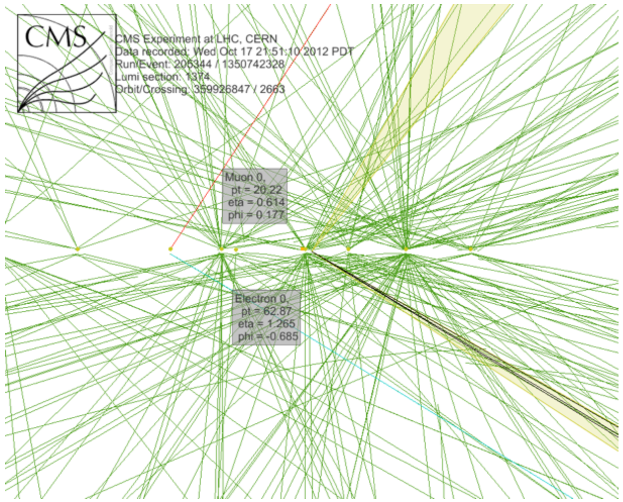

Outline

- Central Exclusive Production
- Exclusive $\gamma\gamma \rightarrow W^+W^-$ production and anomalous quartic gauge couplings: new CMS results at 8 TeV
- CEP at CMS with proton taggers (CT-PPS):
  - Exclusive WW production
  - Exclusive dijet production

Central Exclusive Production

CEP: process of type **pp→ p+X+p**

- **Scattered protons survive the collision intact**
- No additional activity between the outgoing protons and the central system X (exclusive)
- **Particularly clean experimental conditions** thanks to the absence of proton remnants

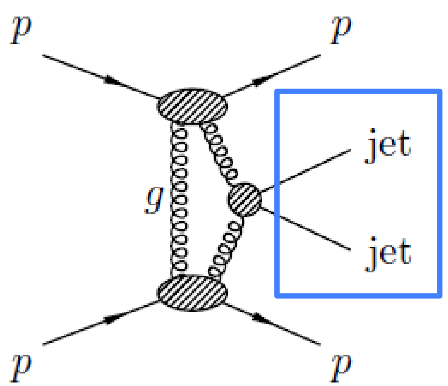

ℙℙ exchanges

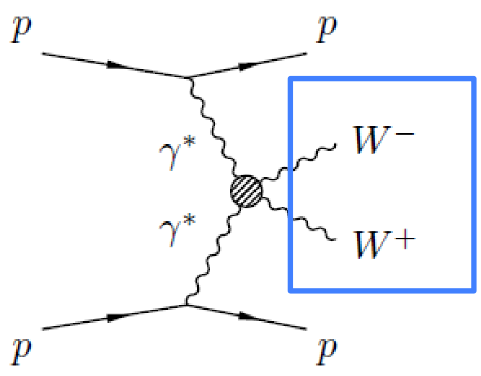

γγ interactions

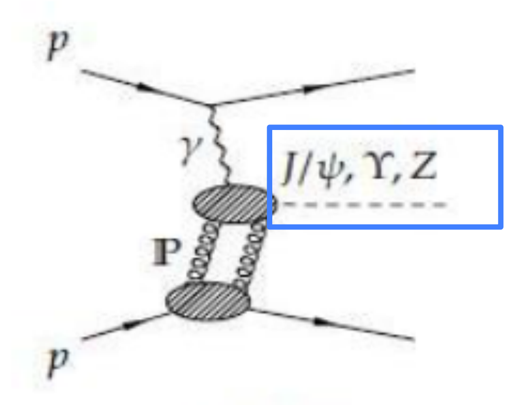

ℙγ fusions

- ✓ Double pomeron exchange: pomeron structure → Marta Ruspa's talk
- ✓ W+W–: study of exclusive processes at high mass and constraint anomalous couplings
- ✓ ℓ+ℓ–: compare to precision QED predictions, calibrate integrated luminosity normalisation and study proton dissociation
- ✓ J/ψ and Υ photo-production: probe gluon distribution at low x

CMS RESULTS

- Search for exclusive or semi-exclusive $\gamma\gamma$ production and observation of exclusive or semi-exclusive e+ e- production in pp collisions at $\sqrt{s}$ = 7 TeV [JHEP 11 (2012) 080]

- Exclusive $\gamma\gamma \to \mu^+\mu^-$ production in proton-proton collisions at $\sqrt{s}$ = 7 TeV [JHEP 01 (2012) 052]

Based on ~ 40 pb^{-1} collected in 2010

- Study of exclusive two-photon production of W^+W^- in pp collisions at $\sqrt{s}$ = 7 TeV [JHEP 07 (2013) 116]

New

- Study of exclusive two-photon production of W^+W^- in pp collisions at $\sqrt{s}$ = 8 TeV [CMS PAS FSQ-13-008]

$\sqrt{s}$ (TeV)	Luminosity (fb^{-1})	Pileup (PU)
7	5	7
8	19.7	21

Results from 8 TeV data analysis shown here

CMS detector

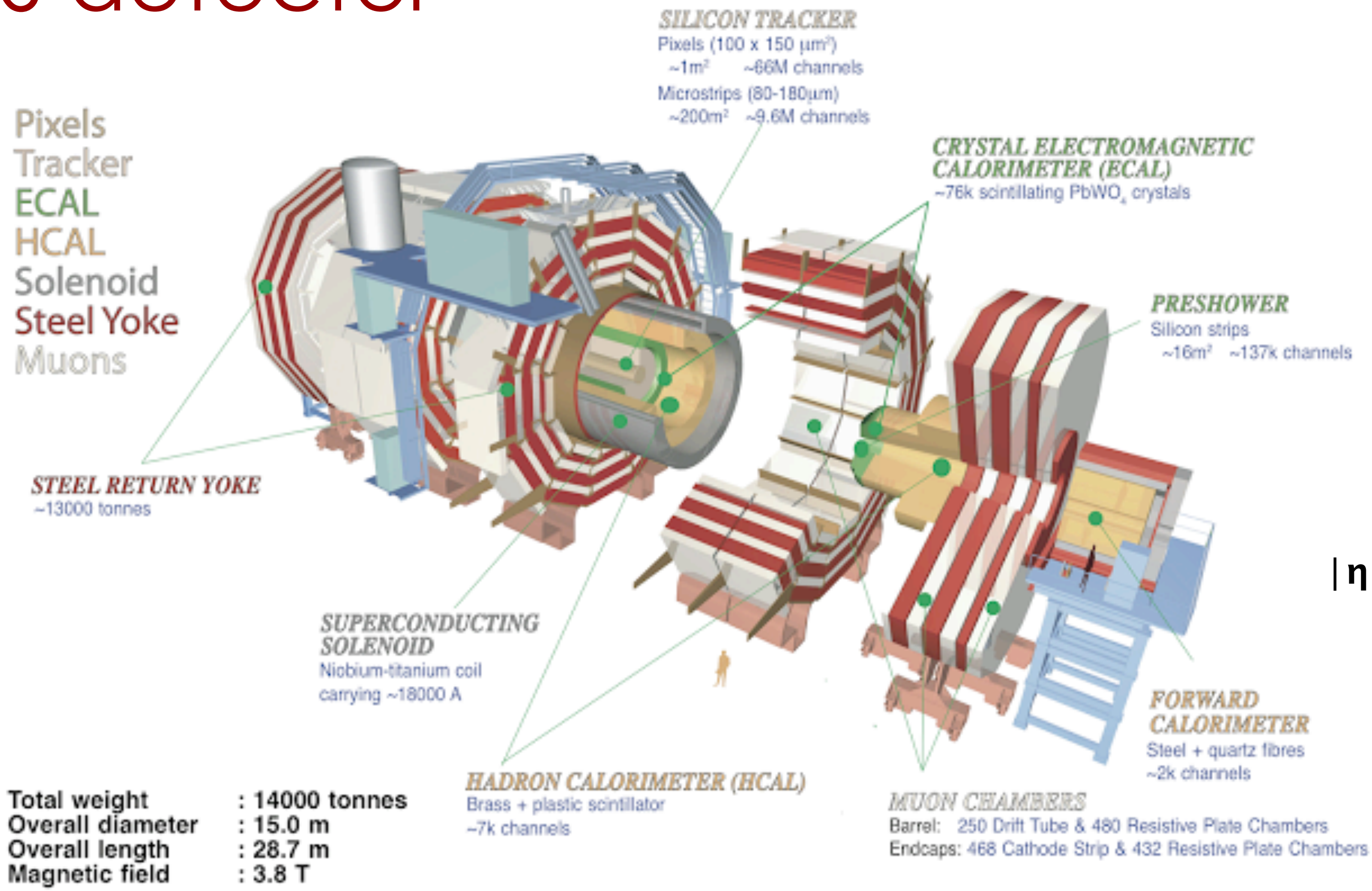

|η| < 5.2

- **BSC, Beam Scintillator Counters :** 3.2 < |η| < 4.7 (in front of the Forward Calorimeter)
- **CASTOR calorimeter:** -6.6 < |η| < -5.2 (14.4 m from IP, one side only)
- **Forward Shower Counters FSC:** 6 < |η| < 8 (59-114 m from IP)
- **Zero Degree Calorimeter:** |η| > 8.1 (140 m from IP)

Forward proton tagging: CT-PPS

The **CMS-TOTEM Precision Proton Spectrometer** (CT-PPS)[1] **will allow precision proton measurements in the very forward regions** on both sides of CMS during standard LCH running**:**

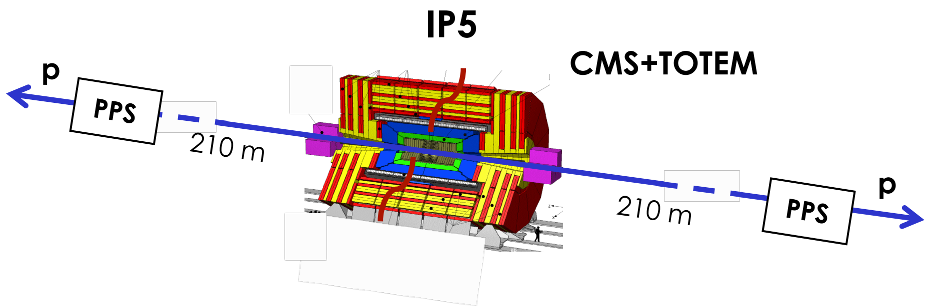

- Two stations for **tracking detectors** and two stations for **timing detectors** installed at ~210 m from the common CMS-TOTEM interaction point (IP5) on both sides of the central apparatus
- LHC magnets between IP5 and the detector stations used to bend out of the beam envelope protons that have lost a small fraction of their initial momentum in the interaction

→ **proton fractional longitudinal momentum loss (ξ) between 2% and 10%**

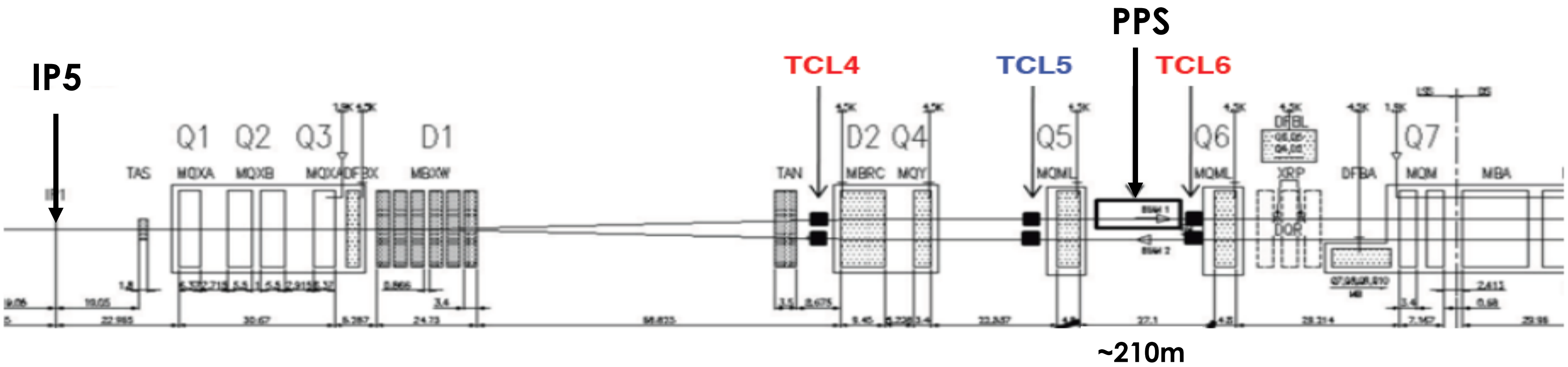

LHC lattice between IP5 and CT-PPS detector stations

[1] CT_PPS TDR, CERN-LHCC-2014-021

CT-PPS design performance and CEP

The measurement of the two scattered protons fully determines the kinematics of the central system X, irrespective of its decay mode.

$$M_X = \sqrt{s \cdot \xi_1 \cdot \xi_2}$$

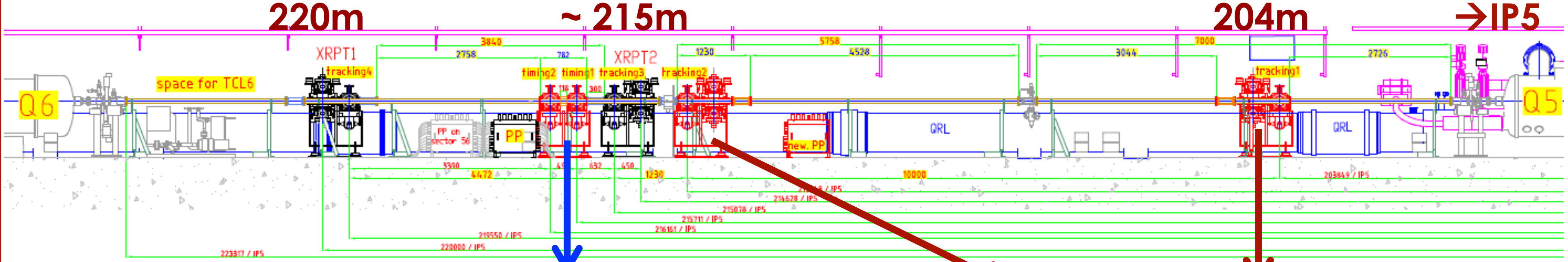

2 new horizontal cylindrical pots equipped with timing detectors

2 horizontal rectangular pots equipped with tracking detectors

Proton timing measurement from both sides of CMS allows to **determine the primary vertex**, correlate it with that of the central detector and **reject pile-up**

- Time resolution ~10 ps
  → **Vertex z-by-timing: ~2 mm**

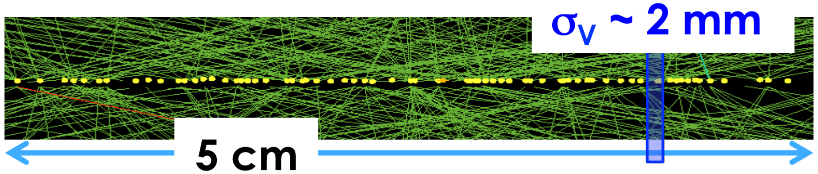

Proton position and angle measurements, combined with the beam magnets, allow to **determine the momentum of the scattered protons**

- Position resolution of ~10 μm
- Angular resolution of ~1-2 μrad
  → **$\Delta p/p$ ~ 2 10^{-4}**
  Mass resolution: ~5 GeV/c^2

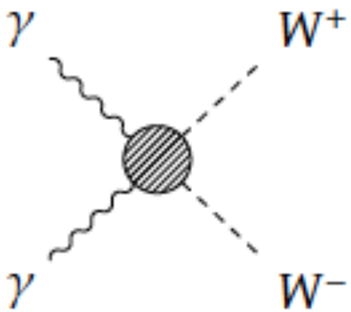

CEP production of W pairs

Theoretical framework

STANDARD MODEL PRODUCTION

SM Lagrangian density contains triple and quartic couplings between γ and W bosons

$$\mathcal{L}^{WW\gamma} = -ie\, F_{\mu\nu} W^{+\mu} W^{-\nu}$$
$$\mathcal{L}^{WW\gamma\gamma} = -e^2 \left(W_\mu^+ W^{-\mu} A_\nu A^\nu - W_\mu^+ W_\nu^- A^\mu A^\nu \right)$$

SM contribution to **γγ** → W^+W^- at leading order:

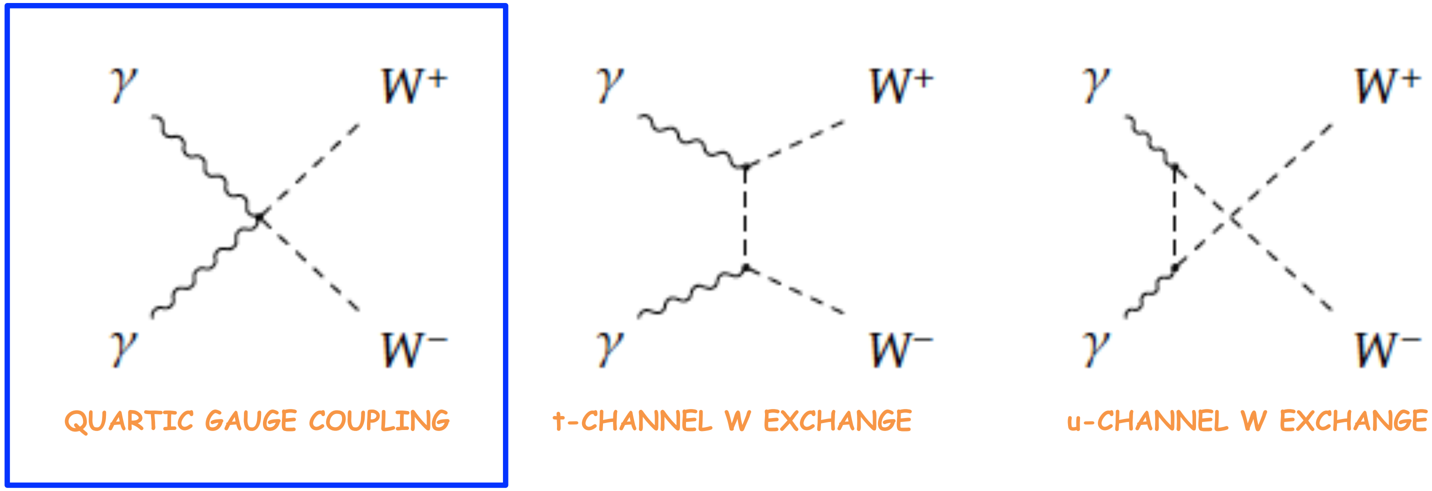

Measurements of the quartic WWγγ coupling can be used to look for any deviation from the SM predictions, which would reveal a sign of new physics.

Theoretical framework

GENUINE ANOMALOUS QUARTIC COUPLINGS (AQGCs)

Potential deviation from SM can be quantified by introducing genuine anomalous quartic couplings (AQGC) of dimension-6 not related to SM triple or quartic couplings [1]

AQGCs introduced via an effective Lagrangian with 2 additional dimension-6 terms:

$$\mathcal{L}_6^0 = \frac{e^2}{8}\frac{a_0^W}{\Lambda^2}F_{\mu\nu}F^{\mu\nu}W^{+\alpha}W^-_\alpha - \frac{e^2}{16\cos^2\Theta_W}\frac{a_0^Z}{\Lambda^2}F_{\mu\nu}F^{\mu\nu}Z^\alpha Z_\alpha$$

$$\mathcal{L}_6^C = \frac{-e^2}{16}\frac{a_C^W}{\Lambda^2}F_{\mu\alpha}F^{\mu\beta}(W^{+\alpha}W^-_\beta + W^{-\alpha}W^+_\beta) - \frac{e^2}{16\cos^2\Theta_W}\frac{a_C^Z}{\Lambda^2}F_{\mu\alpha}F^{\mu\beta}Z^\alpha Z_\beta$$

containing:

- parameters a_0^W and a_C^W
- Λ scale for new physics

A nonlinear representation of the spontaneously broken SU(2)⊗U(1) symmetry assumed

[1] G. Belanger and F. Boudjema, "Probing quartic couplings of weak bosons through three vectors production at a 500-GeV NLC", Phys.Lett. B288 (1992) 201–209,

Theoretical framework

DIMENSION-8 FORMALISM

Assuming a linear representation of the spontaneously broken $SU(2) \otimes U(1)$ symmetry, the lowest-order operators, where new physics may cause deviations in the purely quartic gauge boson couplings, are of dimension 8 [2].

Including the constraint that the $WWZ\gamma$ vertex should vanish, a direct relationship between the dimension-8 $f_{M,0,1,2,3}/\Lambda^4$ couplings and the dimension-6 $a^W_{0,C}/\Lambda^2$ couplings is recovered

$$\frac{a_0^W}{\Lambda^2} = -\frac{4M_W^2}{g^2}\frac{f_{M,0}}{\Lambda^4} - \frac{8M_W^2}{g'^2}\frac{f_{M,2}}{\Lambda^4}$$

$$\frac{a_C^W}{\Lambda^2} = \frac{4M_W^2}{g^2}\frac{f_{M,1}}{\Lambda^4} + \frac{8M_W^2}{g'^2}\frac{f_{M,3}}{\Lambda^4}$$

with $g = \frac{e}{\sin(\theta_W)}$ and $g' = \frac{e}{\cos(\theta_W)}$

[2] M. Baak et al., "Working Group Report: Precision Study of Electroweak Interactions", arXiv:1310.6708.

Theoretical framework

DIPOLE FORM FACTOR

In both the dimension-6 and dimension-8 scenarios, the $\gamma\gamma \rightarrow WW$ cross section in the presence of anomalous couplings increases rapidly with the $\gamma\gamma$ center of mass energy ($W_{\gamma\gamma}$).

→ dipole form factors introduced to preserve unitarity

$$a_{0,C}^{W} \rightarrow a_{0,C}^{W}\left(W_{\gamma\gamma}^{2}\right) = a_{0,C}^{W}\left(1 + \frac{W_{\gamma\gamma}^{2}}{\Lambda_{\text{cutoff}}^{2}}\right)^{-2}$$

Λ_{cutoff} : energy cutoff scale

Two scenarios considered:

- **Λ_{cutoff} = 500 GeV**
- **$\Lambda_{cutoff} \rightarrow \infty$ (no form factor)**

Signal and background contributions

Two contributions to signal:

- elastic production: pp → pW^+W^-p
- proton-dissociative production: pp → $p^*W^+W^-p^*$,

(one or both protons dissociate into a low-mass system that escapes detection)

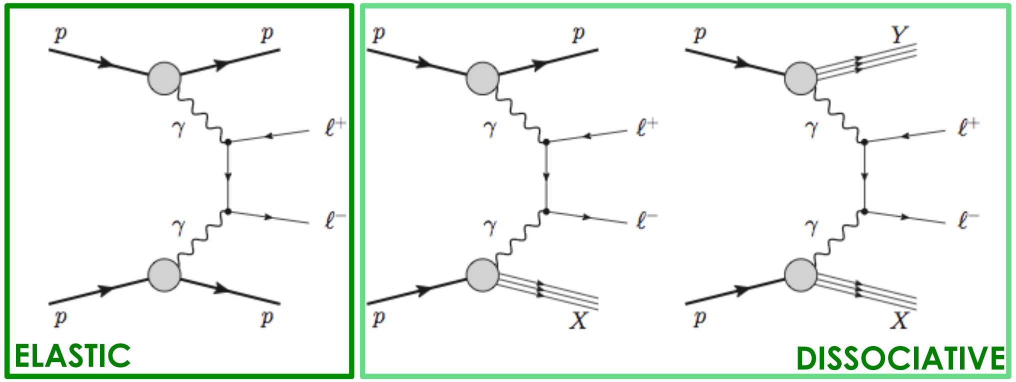

Can not be separated without tagging the forward protons

Background sources:

- Inclusive WW, ttbar, W+jets processes
- ττ pairs produced via the Drell-Yan process
- Exclusive two photon processes: γγ→ll
- WW production from single diffractive interactions
- WW→WW scattering (vector boson fusion)

All backgrounds estimated from Monte Carlo after comparison with data in control regions

Event selection

Unlike-flavor dilepton decay channel: $\gamma\gamma \rightarrow W^+W^- \rightarrow \mu^{\pm}e^{\mp}\nu\bar{\nu}$

(backgrounds due Drell-Yan and two-photon l^+l^- production more than an order of magnitude lower than in the same-flavor final states)

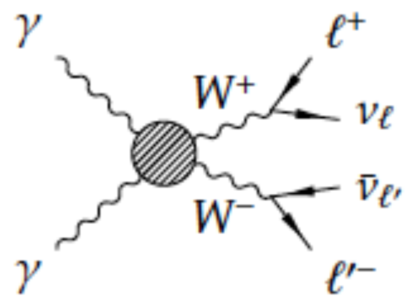

Selection:

- Opposite sign leptons, with p_T>20 GeV and $|\eta|$<2.4, matched to common primary vertex
- No extra tracks associated to the dilepton vertex
- Dilepton invariant mass greater than 20 GeV

SM signal region:

$p_T(\mu e) > 30$ GeV

AQGCs search:

- 2 bins: $p_T(\mu e) = 30\text{-}130$ GeV
  $p_T(\mu e) > 130$ GeV

Signal correction factors

Two effects present in data difficult to describe in simulation:

- mis-association of low p_T, forward tracks from pileup events to dilepton vertex
  → Efficiency of the "zero extra-tracks" cut overestimated in MC
  → Important effect in 8 TeV analysis (PU=21)

- proton dissociation contribution to $\gamma\gamma$ interactions

⇒ **$\gamma\gamma \rightarrow ll$ control samples used to derive correction factors from data**

Zero extra-tracks efficiency correction

Control region dominated by elastic $\gamma\gamma \rightarrow ll$ sample used to estimate the correction to the efficiency of the zero extra-tracks cut

Requiring:

- dilepton vertex with 0 extra tracks
- Z-mass veto
- leptons back-to-back ($1-|\Delta\phi(ll)/\pi|<0.01$)

a deficit in the number of events found in data with respect to simulation

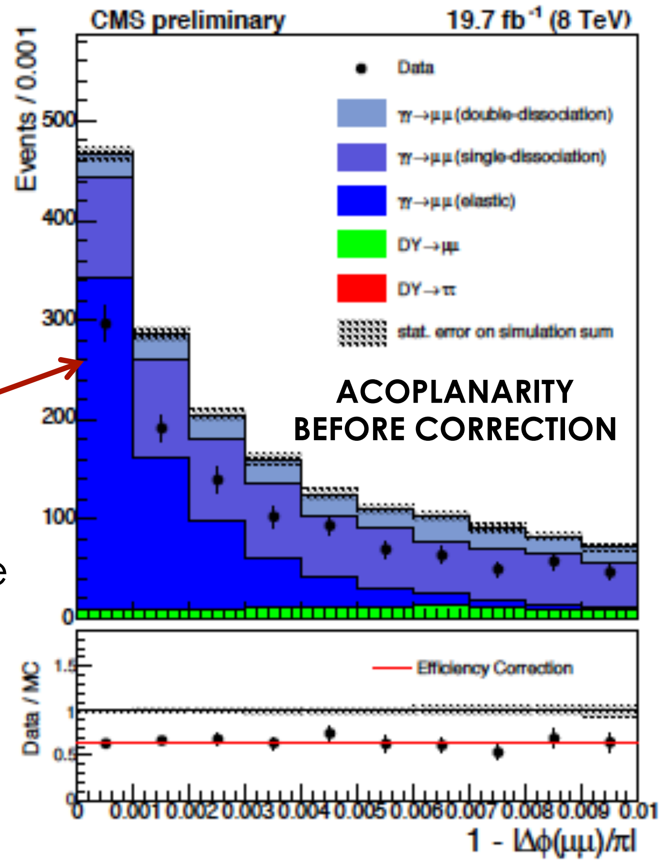

Data/MC in first bin:

0.63 ± 0.04 in $\gamma\gamma \rightarrow \mu\mu$ sample

0.63 ± 0.07 in $\gamma\gamma \rightarrow ee$ sample

This ratio, averaged over the $\mu\mu$ and ee samples, applied to correct the efficiency derived on MC.

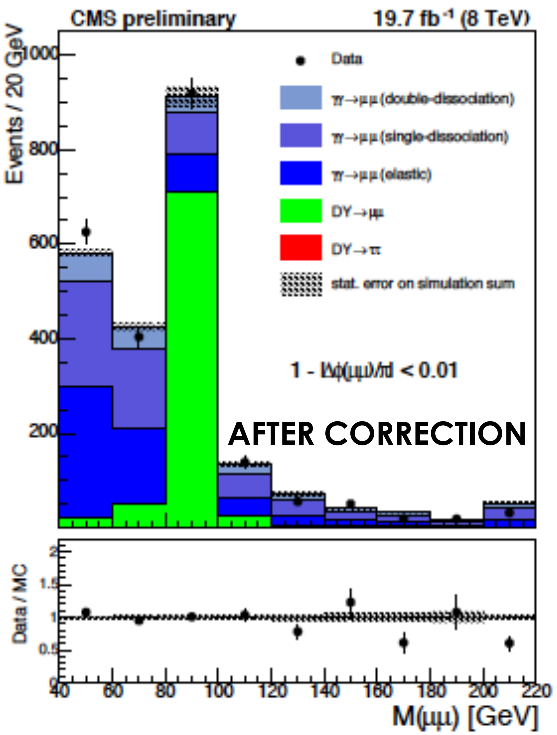

Good data/MC agreement after correction
(checked on several kinematic distributions)

Proton dissociation factor

- Separation of elastic and proton-dissociative events in data not possible without proton tagging
- Simulation of single or double dissociation production difficult (involves soft interactions, only phenomenological models are available)
  → Signal MC samples are purely elastic
- **Strategy**: single/double proton dissociation contribution to $\gamma\gamma\rightarrow WW$ estimated from the data is used to correct MC

Control samples: $\gamma\gamma\rightarrow\mu\mu$ and $\gamma\gamma\rightarrow ee$
- m(ll)>160 GeV
- no extra tracks associated to dilepton vertex

→ Proton dissociation factor $$F = \left[\frac{N_{ll\ data} - N_{DY}}{N_{elastic}}\right]_{m(l^+l^-)>160\,GeV}$$

F=4.10±0.43

Stable as a function of the mass cut in both the dimuon and dielectron channels

F used to correct the elastic pp → pW$^+$W$^-$p prediction to the total pp→p$^{(*)}$ W$^+$W$^-$ p$^{(*)}$ prediction, including proton dissociation

Results – SM signal region

Number of expected signal and background events

Signal	All backgrounds	Inclusive WW	$\gamma\gamma\rightarrow\tau\tau$	DY$\rightarrow\tau\tau$	Diff. WW	Others
5.3±0.1	**3.5±0.5**	**2.0±0.4**	**0.9±0.2**	**0**	**0.1±0.1**	**0.3±0.2**

Mean expected signal significance: 2.4 ± 0.5 σ

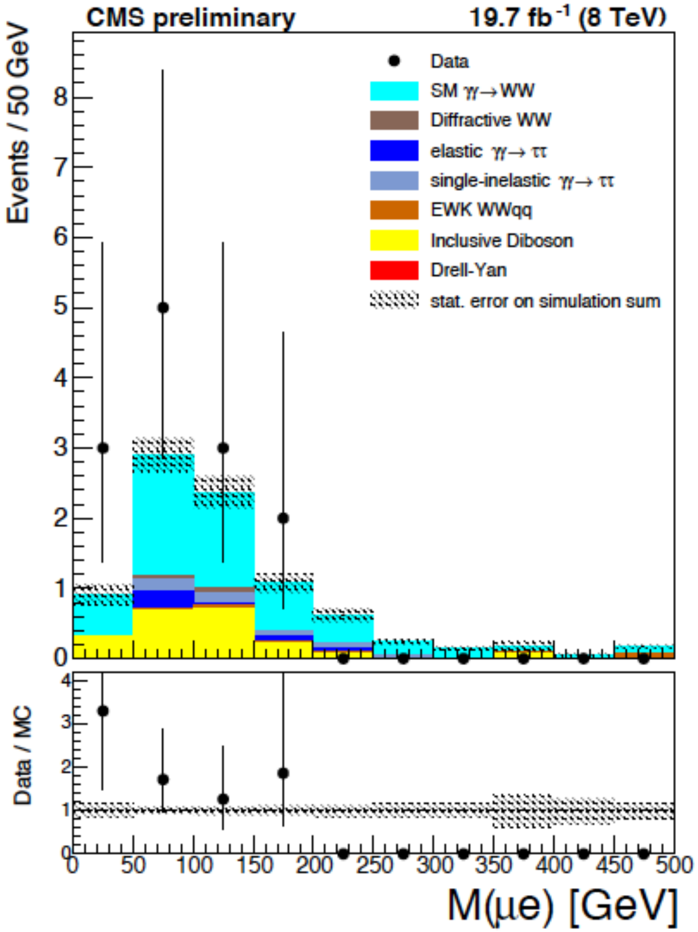

13 events are observed in data that pass all selection criteria

Properties of selected events (μe invariant mass, acoplanarity, missing transverse energy) **consistent with the SM signal plus background prediction**

Cross section measurement:

$$\sigma(pp \rightarrow p^{(*)}W^+W^-p^{(*)} \rightarrow p^{(*)}\mu^\pm e^\mp p^{(*)}) = 12.3^{+5.5}_{-4.4}\text{fb}$$

SM prediction: 6.9 ± 0.6 fb

Observed significance above the background-only hypothesis: 3.6 σ (systematic uncertainties included)

Results – anomalous couplings (I)

- **No significant deviation from SM observed** in the $p_T(\mu e)$ distribution
- **95% CL limits on a^W_0/Λ^2 and a^W_C/Λ^2** derived using Feldman-Cousins prescription with systematic uncertainties treated as log-normal nuisance parameters, for 2 scenarios:

		OPAL (2004)	DØ (2013)	CMS (2013)	CMS(2015)
$a_0^W/\Lambda^2[GeV^{-2}]$	no form factor	$\pm 2\times 10^{-2}$	$\pm 4.3\times 10^{-4}$	$\pm 4.0\times 10^{-6}$	$\pm 1.2\times 10^{-6}$
	Λ_{cutoff} = 500 GeV		$\pm 2.5\times 10^{-3}$	$\pm 1.5\times 10^{-4}$	$(-1.1\ -\ 1.0)\times 10^{-4}$
$a_C^W/\Lambda^2[GeV^{-2}]$	no form factor	${}^{+3.7}_{-5.2}\times 10^{-2}$	$\pm 1.5\times 10^{-3}$	$\pm 1.5\times 10^{-5}$	$\pm 4.4\times 10^{-6}$
	Λ_{cutoff} = 500 GeV		$\pm 9.2\times 10^{-3}$	$\pm 5.0\times 10^{-4}$	$(-4.2\ -\ 3.4)\times 10^{-4}$
				$\sqrt{s}=7\ TeV$	$\sqrt{s}=8\ TeV$

✓ Up to two orders of magnitude improvement to limits set by previous experiments

✓ **Λ_{cutoff} = 500 GeV → 8 TeV limit ~25% better than 7 TeV limit**

✓ **No form factor → 8 TeV limit ~3 times better than 7 TeV limit**

Results – anomalous couplings (II)

Similar statistical procedure used to derive **two dimensional limits in the a^W_0/Λ^2, a^W_C/Λ^2 parameter space with Λ_{cutoff} = 500 GeV**.

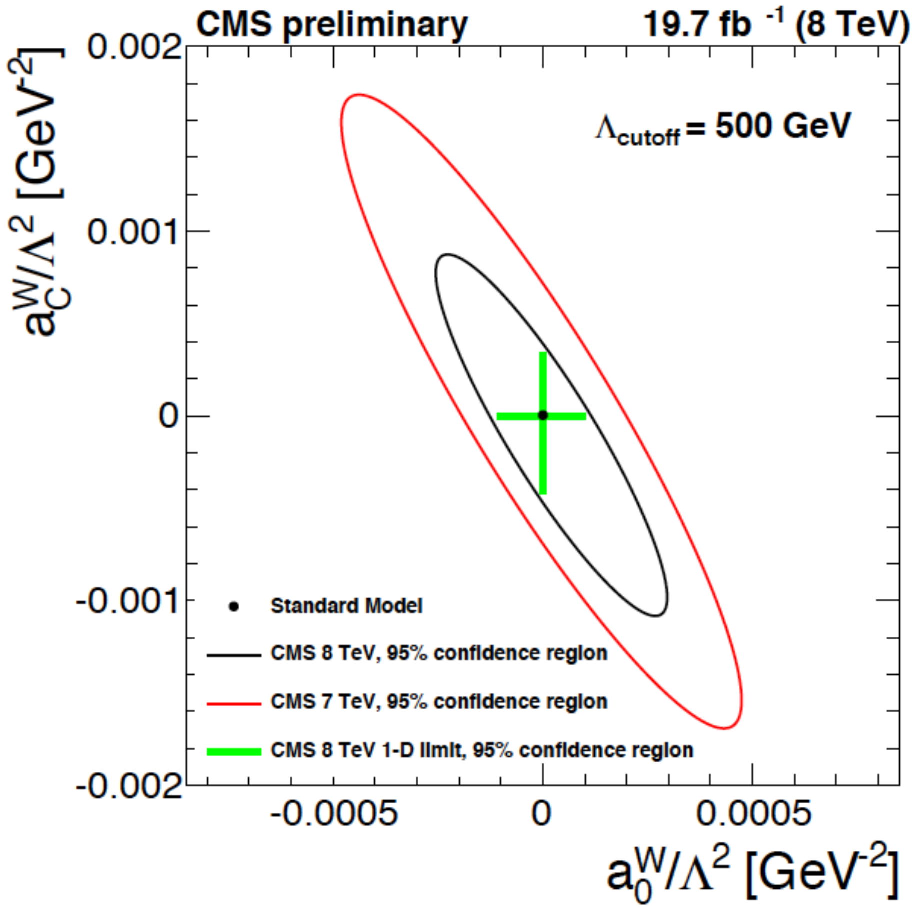

The area outside the solid contour excluded by this measurement at 95% CL

Results – anomalous couplings (III)

The transformed dimension-8 limits derived from a^W_0/Λ^2 and a^W_C/Λ^2:

With Form Factor, cutoff = 500 GeV

$$-4.2\times10^{-10} < f_{M,0}/\Lambda^4 < 3.8\times10^{-10}\,GeV^{-4}$$
$$-16\times10^{-10} < f_{M,1}/\Lambda^4 < 13\times10^{-10}\,GeV^{-4}$$
$$-2.1\times10^{-10} < f_{M,2}/\Lambda^4 < 1.9\times10^{-10}\,GeV^{-4}$$
$$-8.0\times10^{-10} < f_{M,3}/\Lambda^4 < 6.6\times10^{-10}\,GeV^{-4}$$

No Form Factor

$$-4.6\times10^{-12} < f_{M,0}/\Lambda^4 < 4.6\times10^{-12}\,GeV^{-4}$$
$$-17\times10^{-12} < f_{M,1}/\Lambda^4 < 17\times10^{-12}\,GeV^{-4}$$
$$-2.3\times10^{-12} < f_{M,2}/\Lambda^4 < 2.3\times10^{-12}\,GeV^{-4}$$
$$-8.5\times10^{-12} < f_{M,3}/\Lambda^4 < 8.5\times10^{-12}\,GeV^{-4}$$

7-16 times more stringent than previous CMS limits on 8-dimensional parameters:

"A Search for WWγ and WZγ production in pp Collisions at √s = 8 TeV"
[CMS-PAS-SMP-13-009]

Observed Limits
-77 (TeV^{-4}) < $f_{M,0}/\Lambda^4$ < 81 (TeV^{-4})
-131 (TeV^{-4}) < $f_{M,1}/\Lambda^4$ < 123 (TeV^{-4})
-39 (TeV^{-4}) < $f_{M,2}/\Lambda^4$ < 40 (TeV^{-4})
-66 (TeV^{-4}) < $f_{M,3}/\Lambda^4$ < 62 (TeV^{-4})

CEP in Run2 with CT-PPS

With the integrated luminosity expected in Run2 and the CT-PPS detector, the experimental reach of CMS can be extended. It will be possible to:

- improve current limits (e.g. on AQGC) by several orders of magnitude
- study new processes
- search for new physics

For the CT-PPS TDR two processes studied in detail

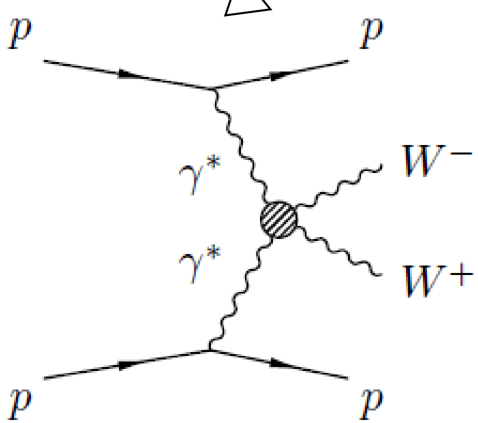

Exclusive WW production

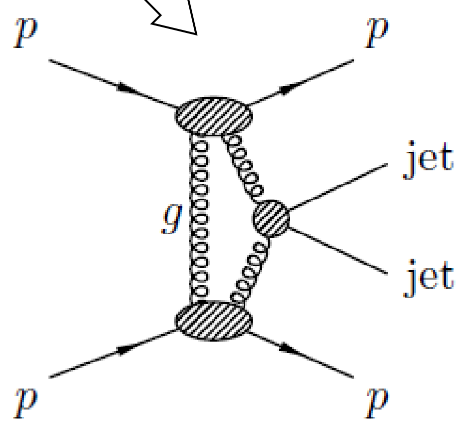

Exclusive dijet production

For these studies events generated at √s=13 TeV

Exclusive WW production (TDR study)

Study only **eμ final state**

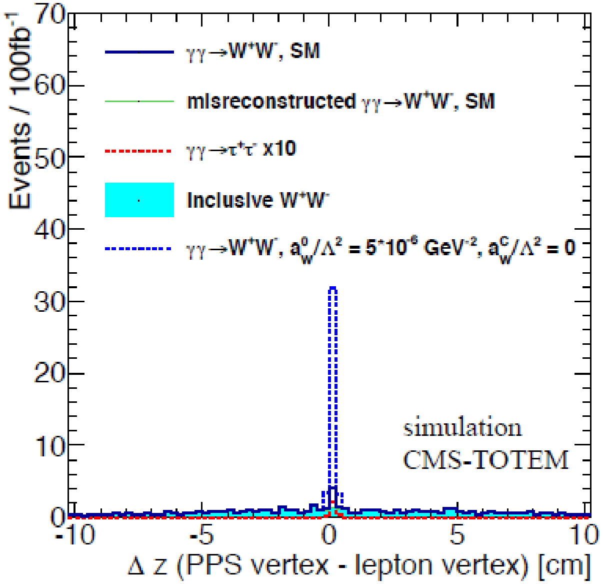

Proton timing is a powerful tool **to reject background**

Timing resolution of **10 ps** is assumed

Track multiplicity associated to the dilepton vertex after the timing selection cut

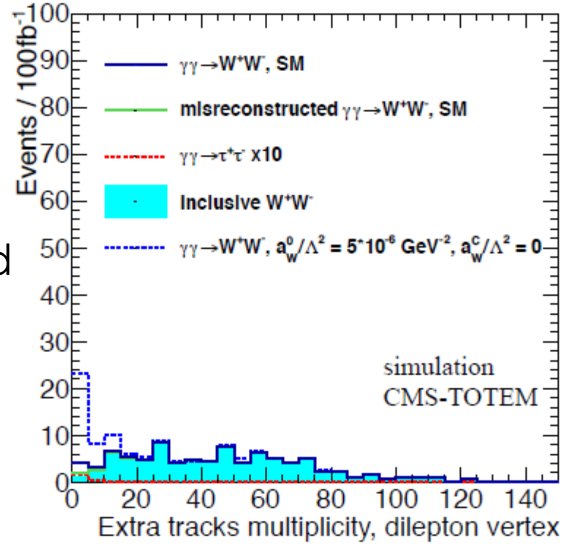

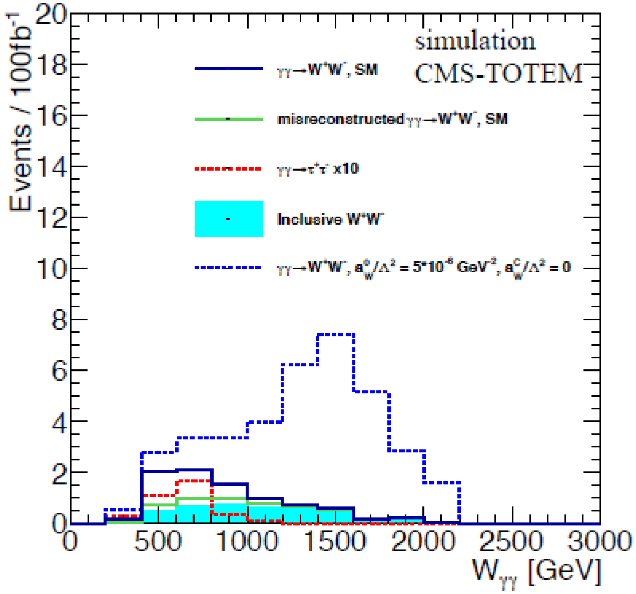

Tail of the $W_{\gamma\gamma}$ distribution ($W_{\gamma\gamma} = M_X = \sqrt{s \cdot \xi_1 \cdot \xi_2} > 1$ TeV), where SM contribution is expected to be small, provides a very **clear separation of AQGC events**

AQGC expected limits with CT-PPS

Expected two dimensional limits in the a^W_0 / Λ^2, a^W_C / Λ^2 parameter space @95%CL:

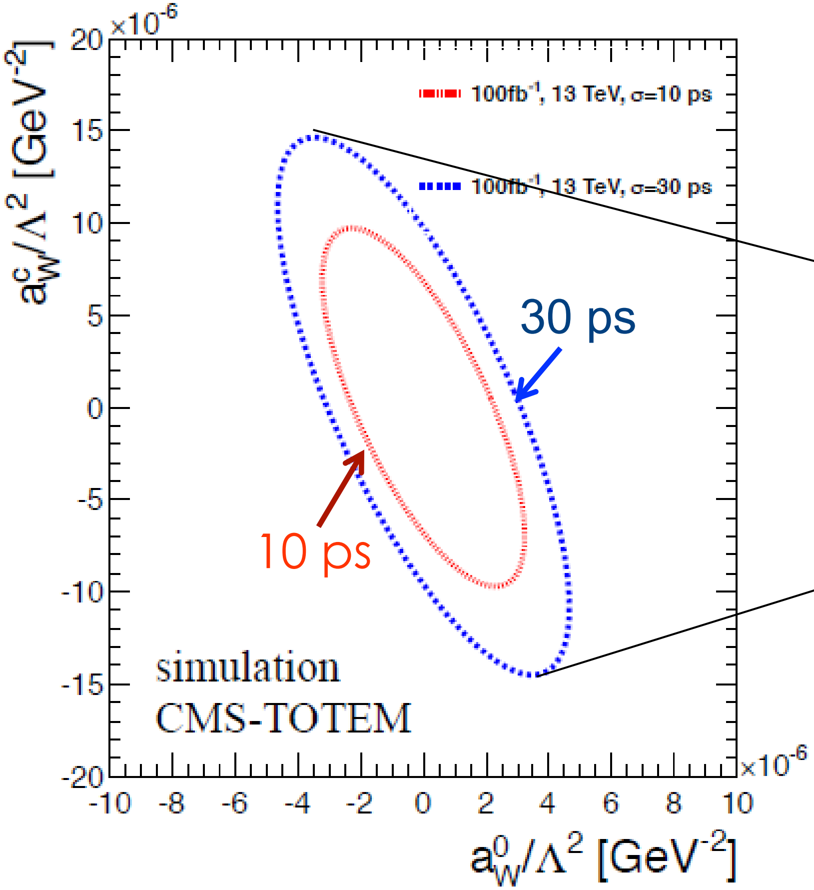

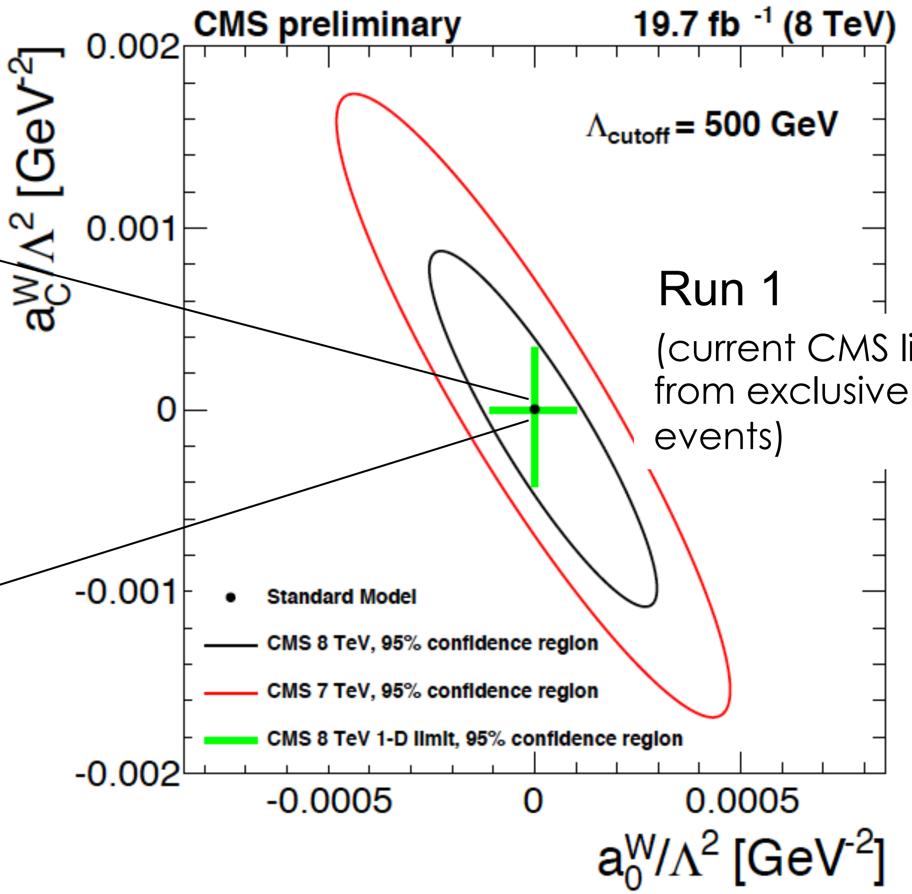

Run 1

(current CMS limits from exclusive WW events)

Exclusive dijet production (TDR study)

Require 2 jets with p_T>100 GeV and $|\eta|$<2

PPS vertex vs vertex of leading jet

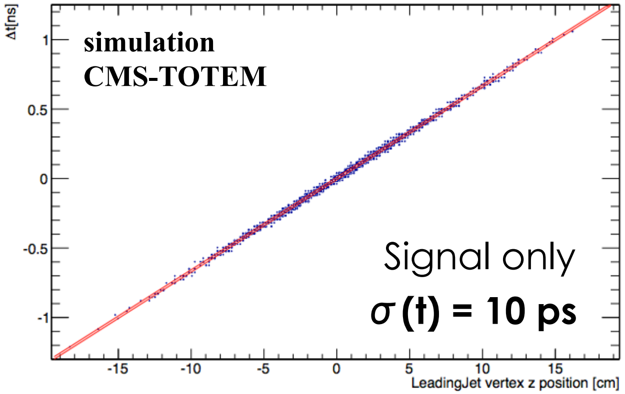

Proton timing as powerful discriminant for exclusive states:

- retain ~66% (1σ) of signal
- rejects ~70% of QCD bkg

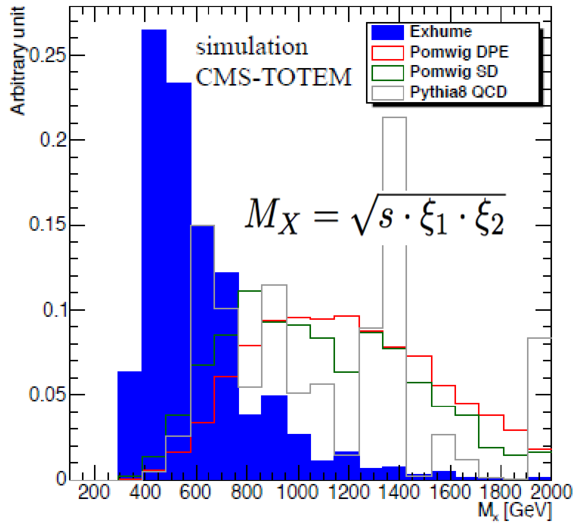

Exclusivity cuts

Dijet mass fraction:

$$\frac{M_{jj}\text{ (central detector)}}{M_X\text{ (PPS)}}$$

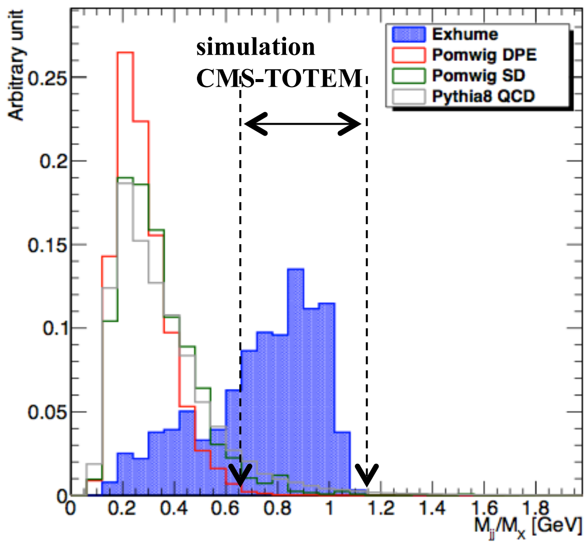

Rapidity difference:

y_{jj} (central detector) – y_X (PPS)

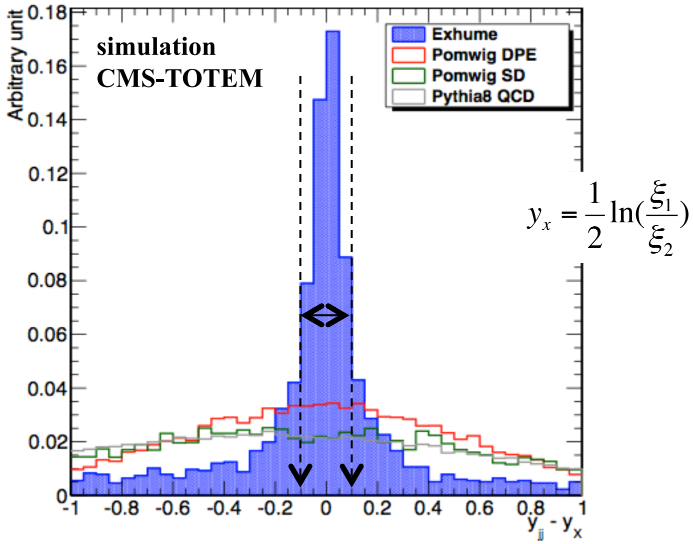

Expected dijet yields (1fb^{-1} - Pileup=25)

Event yields for signal and background processes as a function of the cuts applied.

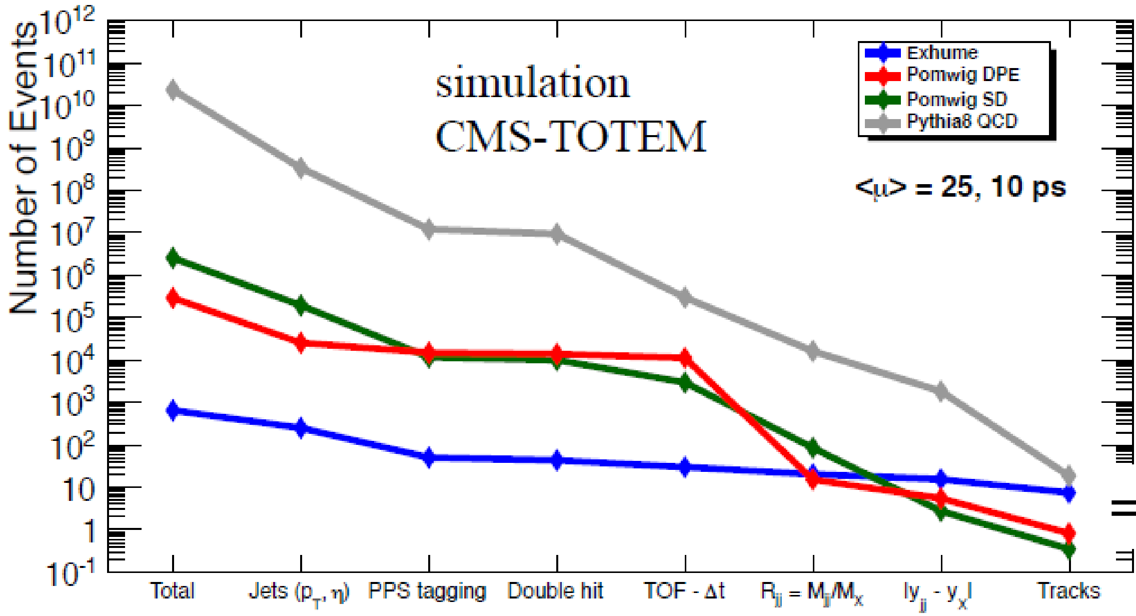

⇒ S/B ~ 1/3

	Exclusive dijets	DPE	SD	Inclusive dijets	S:B
pileup $\mu = 25$					
$M_X \leq 500$ GeV	4.0±0.2	0.2±0.1	0±1	1 ± 1	3:1
$500 < M_X \leq 800$ GeV	3.1±0.2	0.3±0.1	0±1	15 ± 1	1:5
$M_X > 800$ GeV	0.3±0.1	0.3±0.1	1±1	4 ± 1	1:18

Summary

- Central Exclusive Production allows to study a **variety of physics topics**.

- **New CMS results for $\gamma\gamma \rightarrow$ WW exclusive production at 8 TeV** presented:
  - 13 events are observed; their properties consistent with the SM signal plus background prediction
  - Cross section measurement
  - More stringent limits on AQGCs

- Prospects for CEP measurements with CT-PPS discussed:
  precision proton tracking and timing detectors in the very forward region to study CEP in **standard LHC running at high luminosity**

  Project planning: **detector installation in 2016**
  aim at accumulating 100 fb^{-1} of data before LHC LS2

Backup

Signal region

SM signal

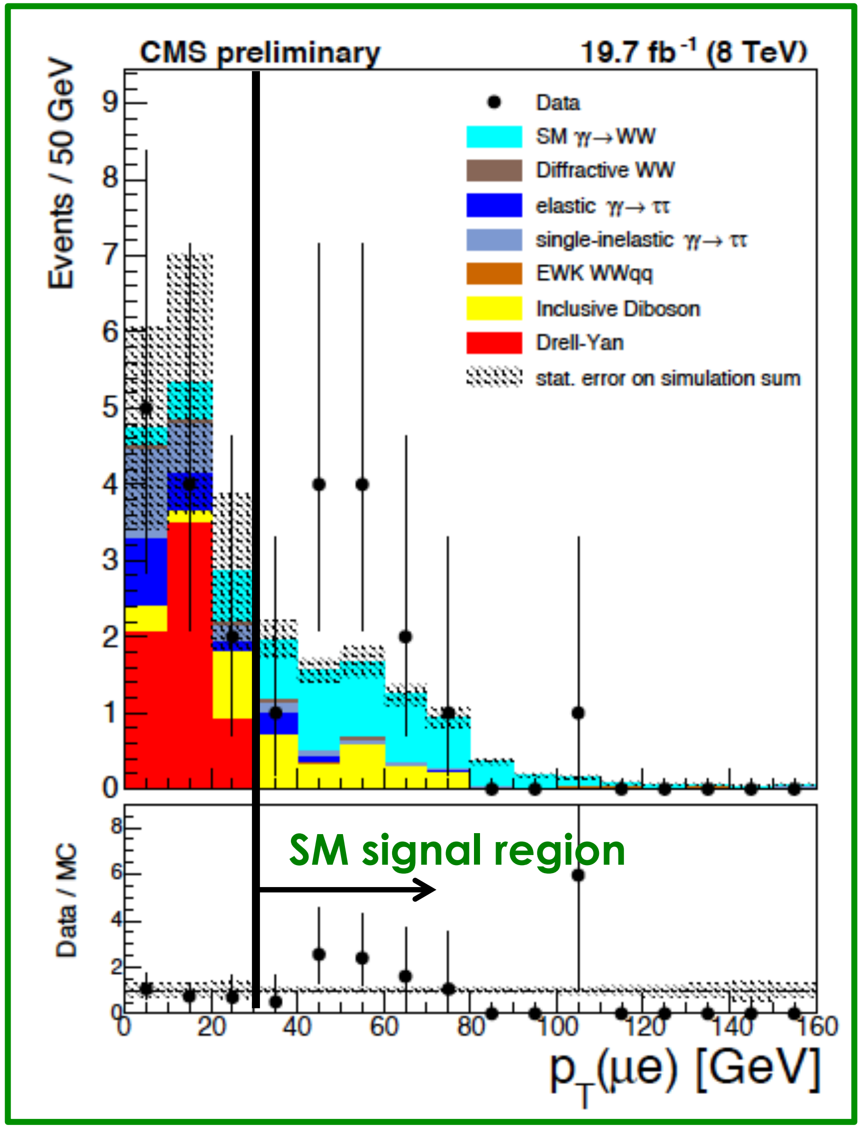

AQGCs search

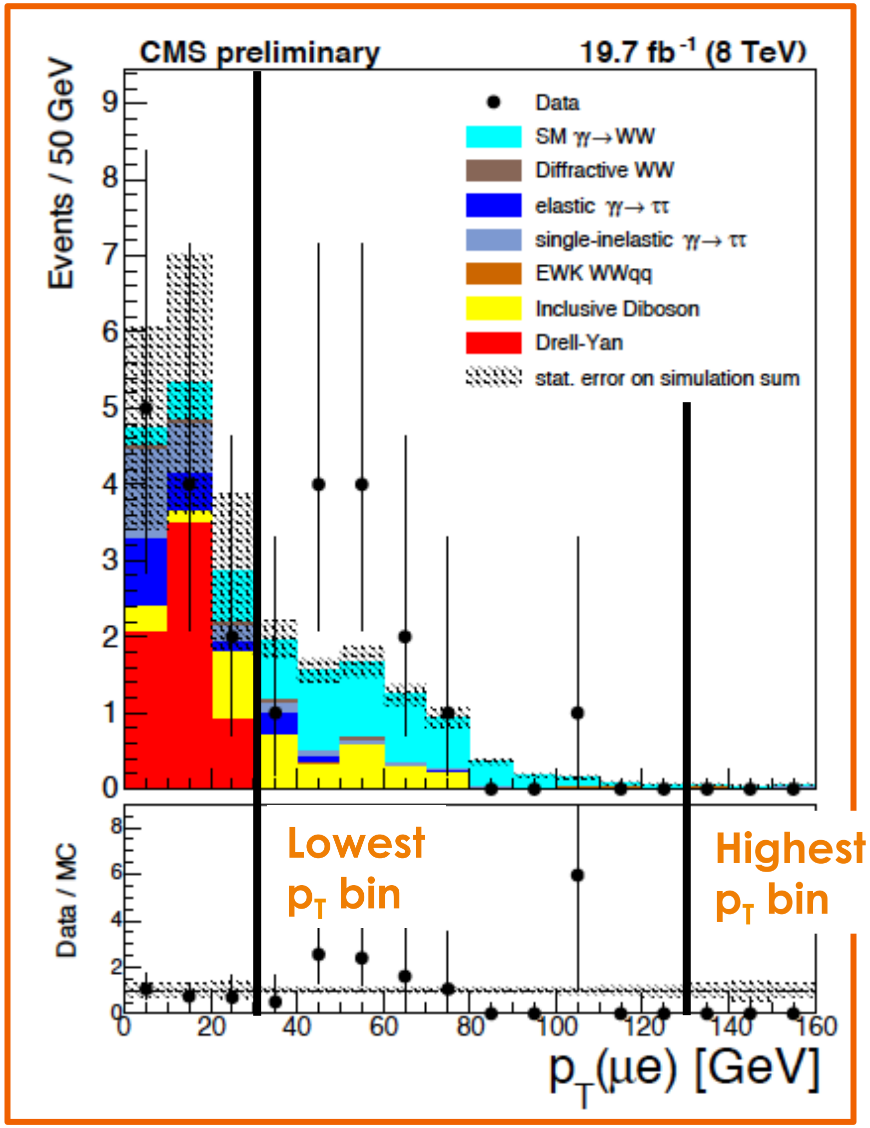

Muon-electron transverse momentum for events which pass all the selection criteria

CT-PPS MC simulation ($\sqrt{s}$=13 TeV)

- **$\gamma\gamma \rightarrow$WW**
  - ✓Events generated with FPMC (V1.0)
  - ✓HERWIG (v6.5) used to simulate the WW pair decay
  - ✓Events generated in the region $0<|t|<4$ GeV^2 and $0.01<\xi<0.2$

- **pp→pJJp**
  - ✓Events generated with ExHuME (V1.3.2, but GSP 5%) interfaced with PYTHIA (v6.426)

- **Backgrounds**
  - ✓SD+DPE events generated with POMWIG (v2.0) interfaced with HERWIG (v6.521)
  - ✓Multijet QCD events simulated with PYTHIA (v8.175)
  - ✓Inclusive WW events simulated with PYTHIA (v6.426)
  - ✓Exclusive $\gamma\gamma \rightarrow \tau\tau$ generated with FPMC

- **Pileup** incorporated by simulating additional interactions with an average pileup multiplicity of μ=50. Minimum bias events generated with
  - ✓PYTHIA (v6.175) for exclusive WW analysis
  - ✓PYTHIA (v8.4) for exclusive dijets analysis

  mixed to signal events

- **Particle transport** from the IP to the CT-PPS detector location performed with HECTOR

Generator-level distributions of | t | and ξ

Signal and background events in the exclusive dijet (top) and exclusive WW (bottom) samples.

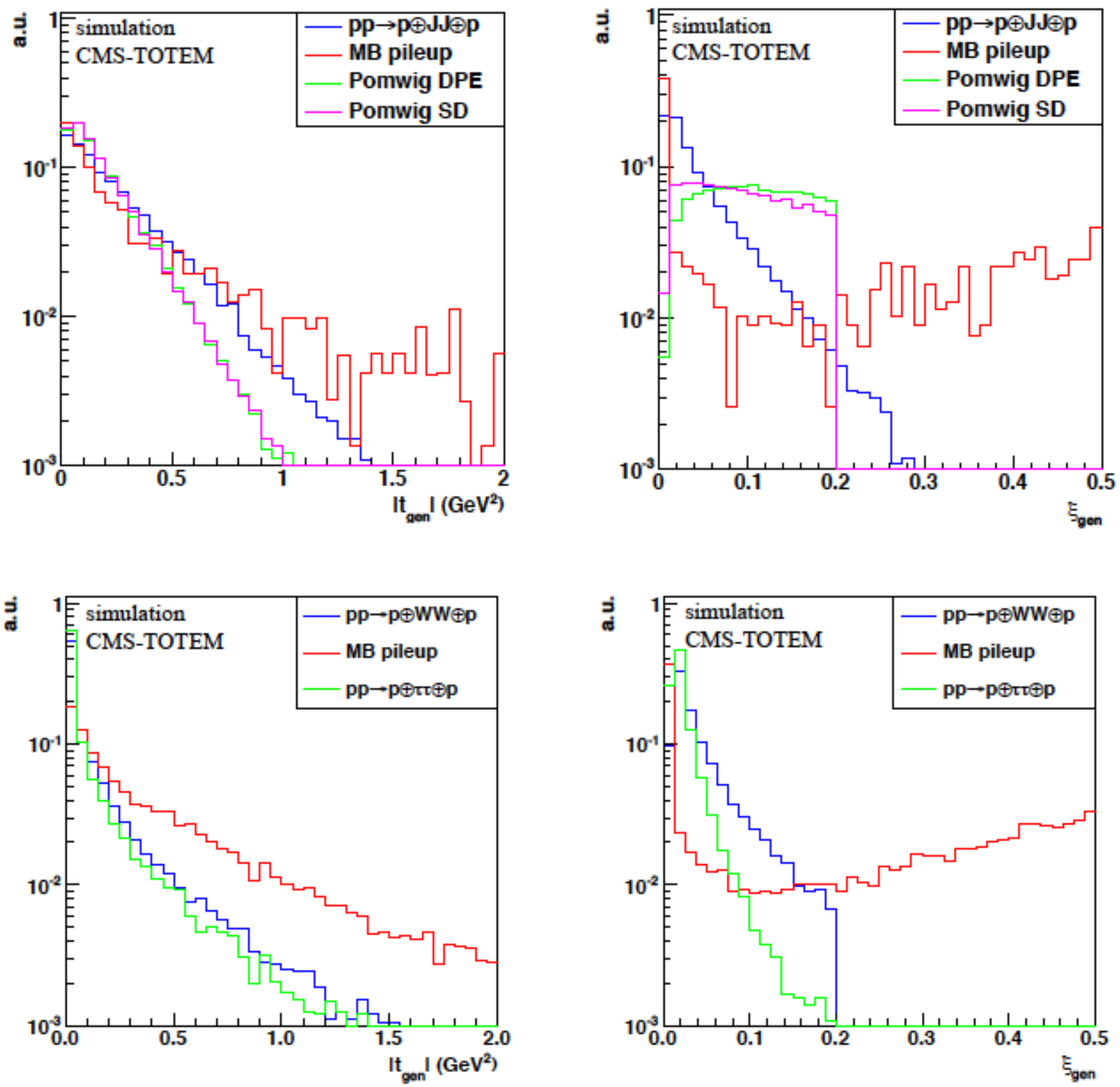

Generator-level distributions of | t | and ξ

Signal and background events in the exclusive dijet and exclusive WW samples.

Coincidence of hits in the 2 tracking stations required.

Tracking detectors located at a distance of 15 σ from the beam center.

Smearing effects due to

- vertex position,
- beam energy dispersion
- crossing angle

accounted for.

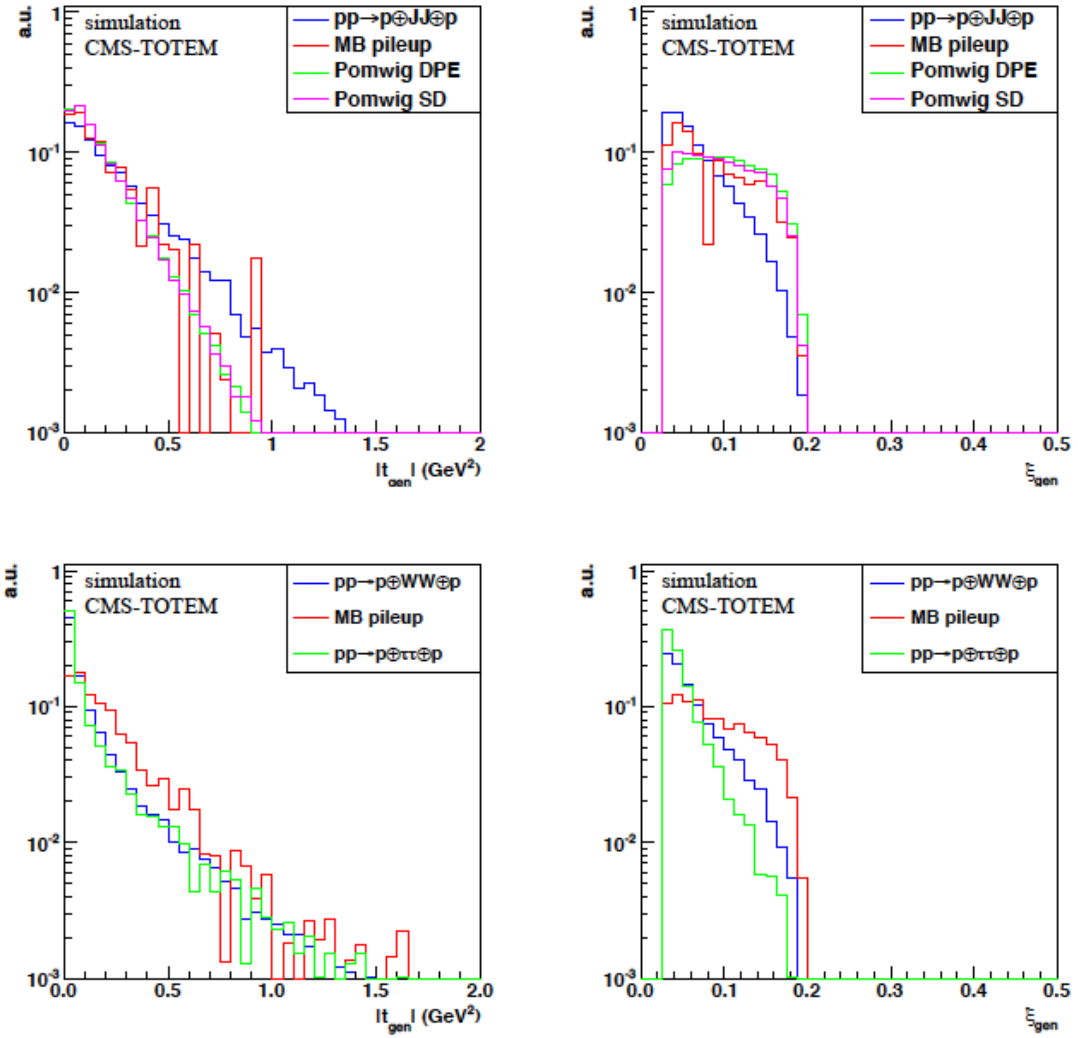

Horizontal beam size

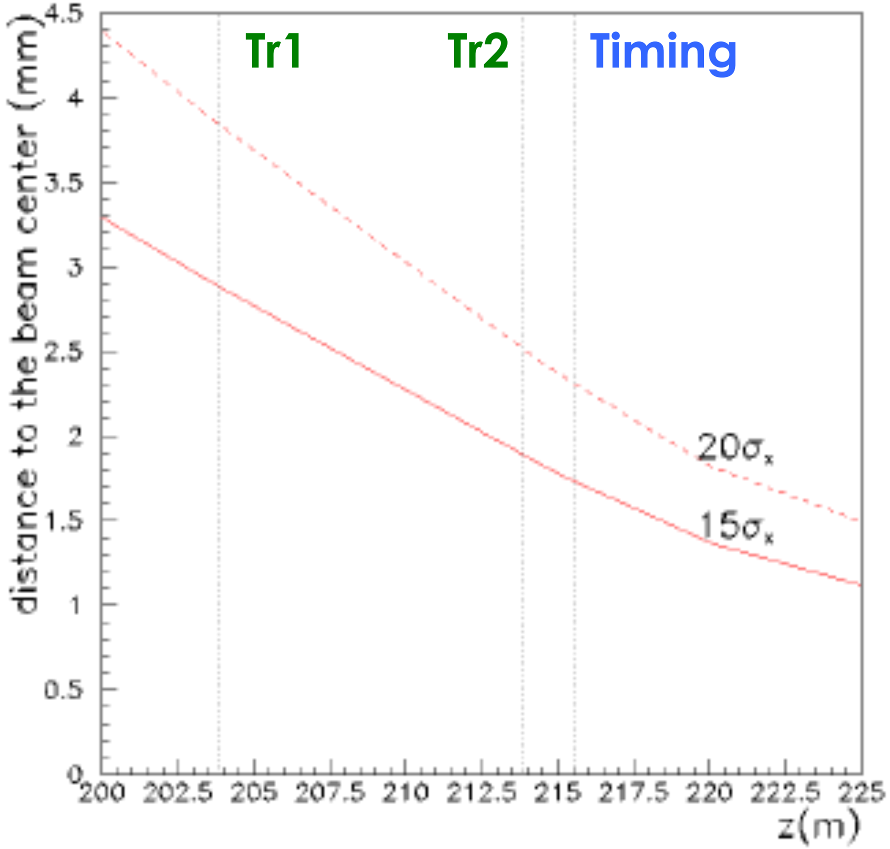

Amplitude function @ IP (β*): 0.6 m

Emittance (ε): 5.4 10^{-10} m

Crossing angle: 142.5 μrad (horizontal plane)

Vertex resolution of $\sigma^*_{x,y}$ = 15 μm

Angular beam divergence @ IP : 30 μrad

Detector acceptance

“Particle gun” sample: protons generated at fixed (|t|, ξ) transported from IP to CT-PPS detector location with HECTOR.

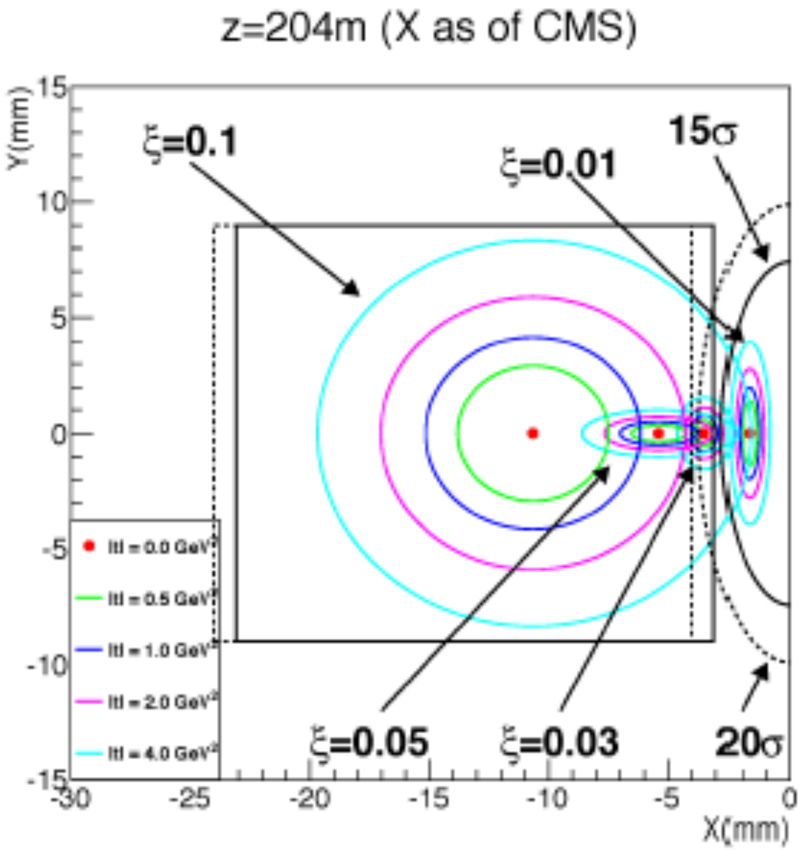

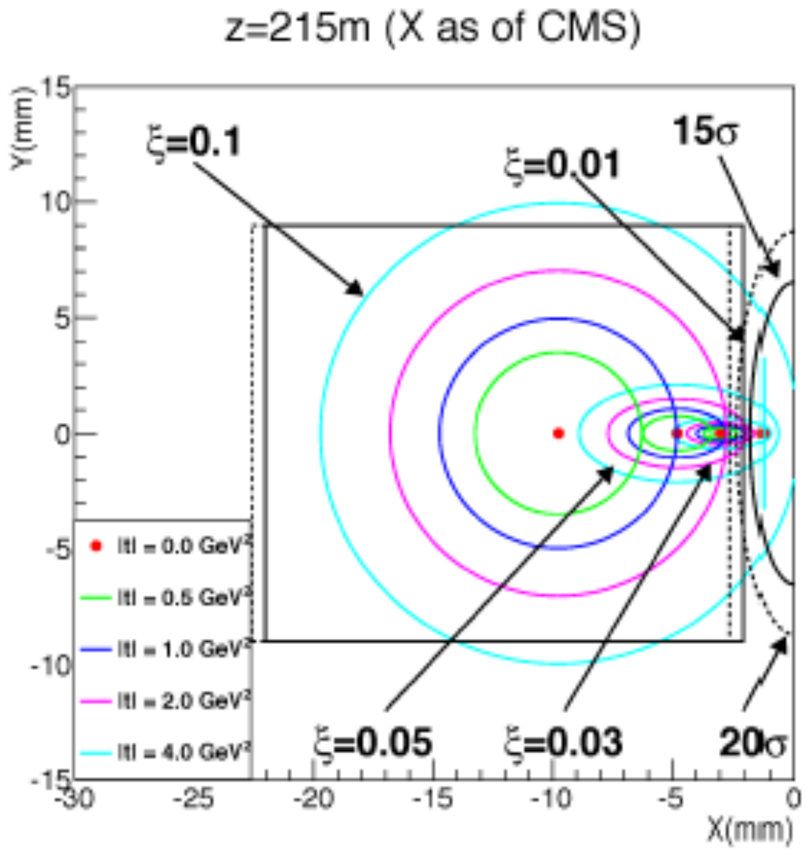

Hit distribution

Hit distributions for centrally produced exclusive dijet and WW events for the tracking detectors located at z=204 m.

Beam energy, vertex smearing and detector resolution are accounted for.

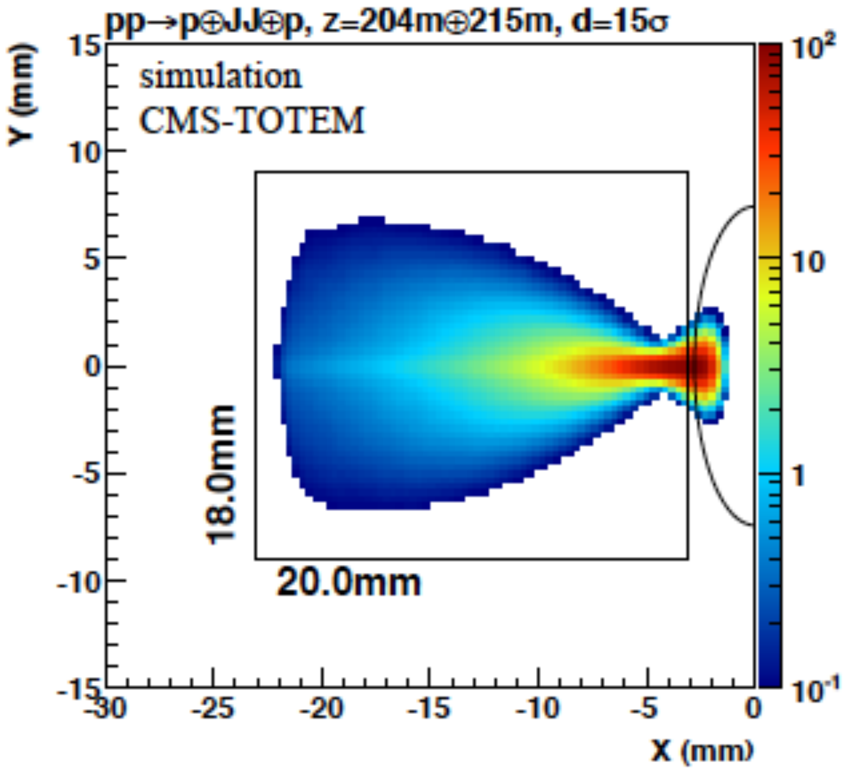

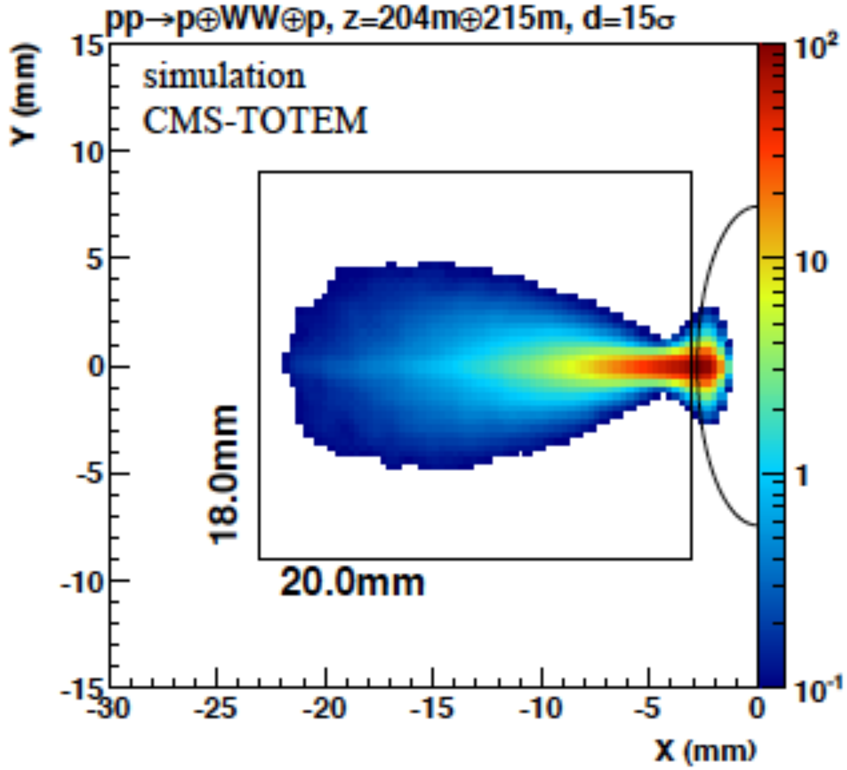

Detector acceptance: |t| and ξ

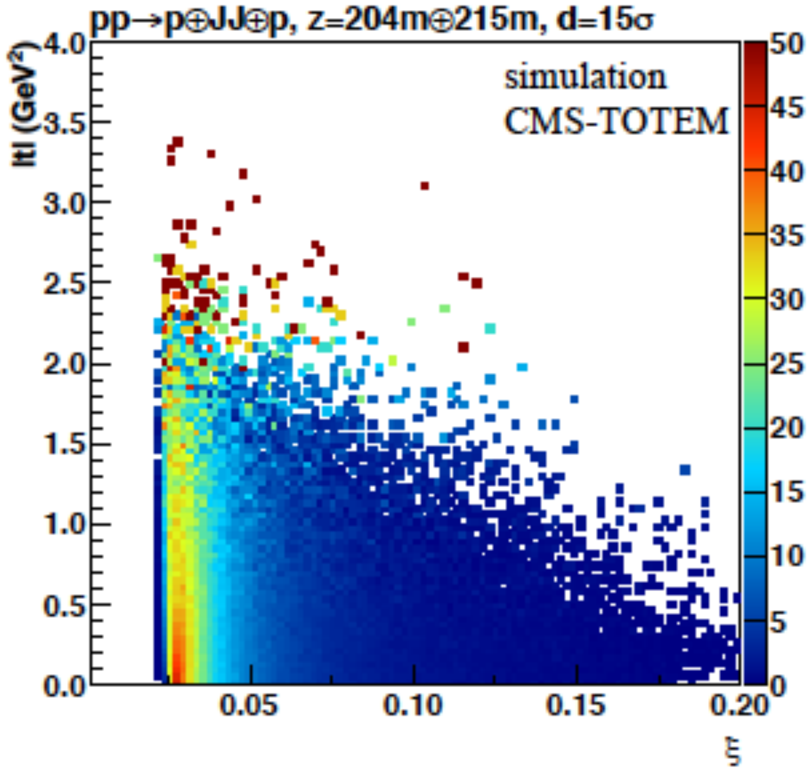

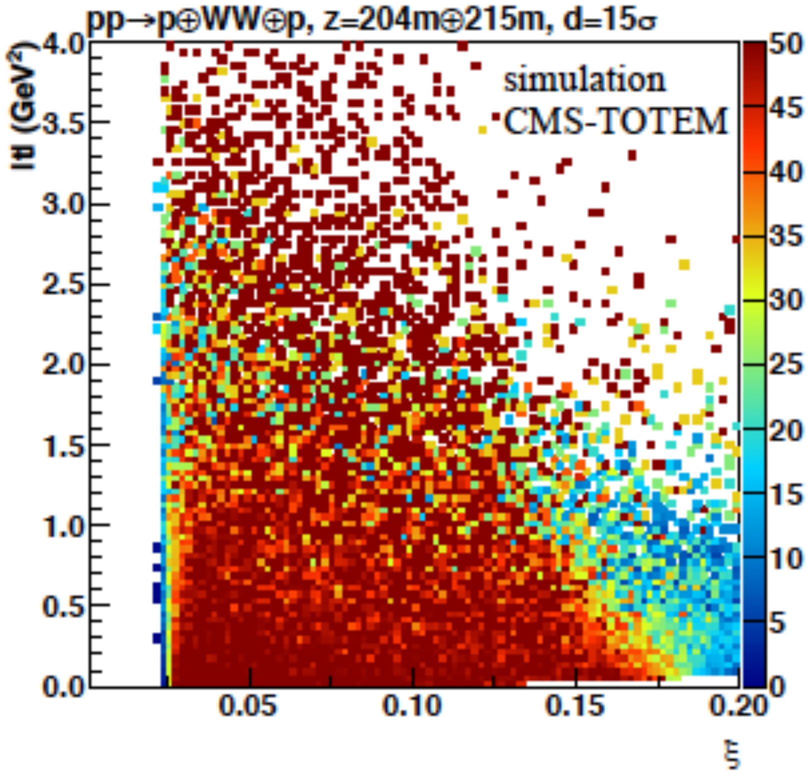

Coincidence of hits in the tracking stations at z=204 m and z=215 m on both sides of the IP required

M_X acceptance and resolution

- With detectors at 15σ from the beam centre, PPS selects exclusive systems in the 350-1700 GeV range (ε>5%)

⇩

Search for exclusive (light) Higgs production is not possible

- At 15σ acceptance larger wrt 20σ for lower mass range
- γγ central system acceptance greater than that for gluon-gluon events because of smaller |t|
- Mass resolution ~1.5% at 500 GeV

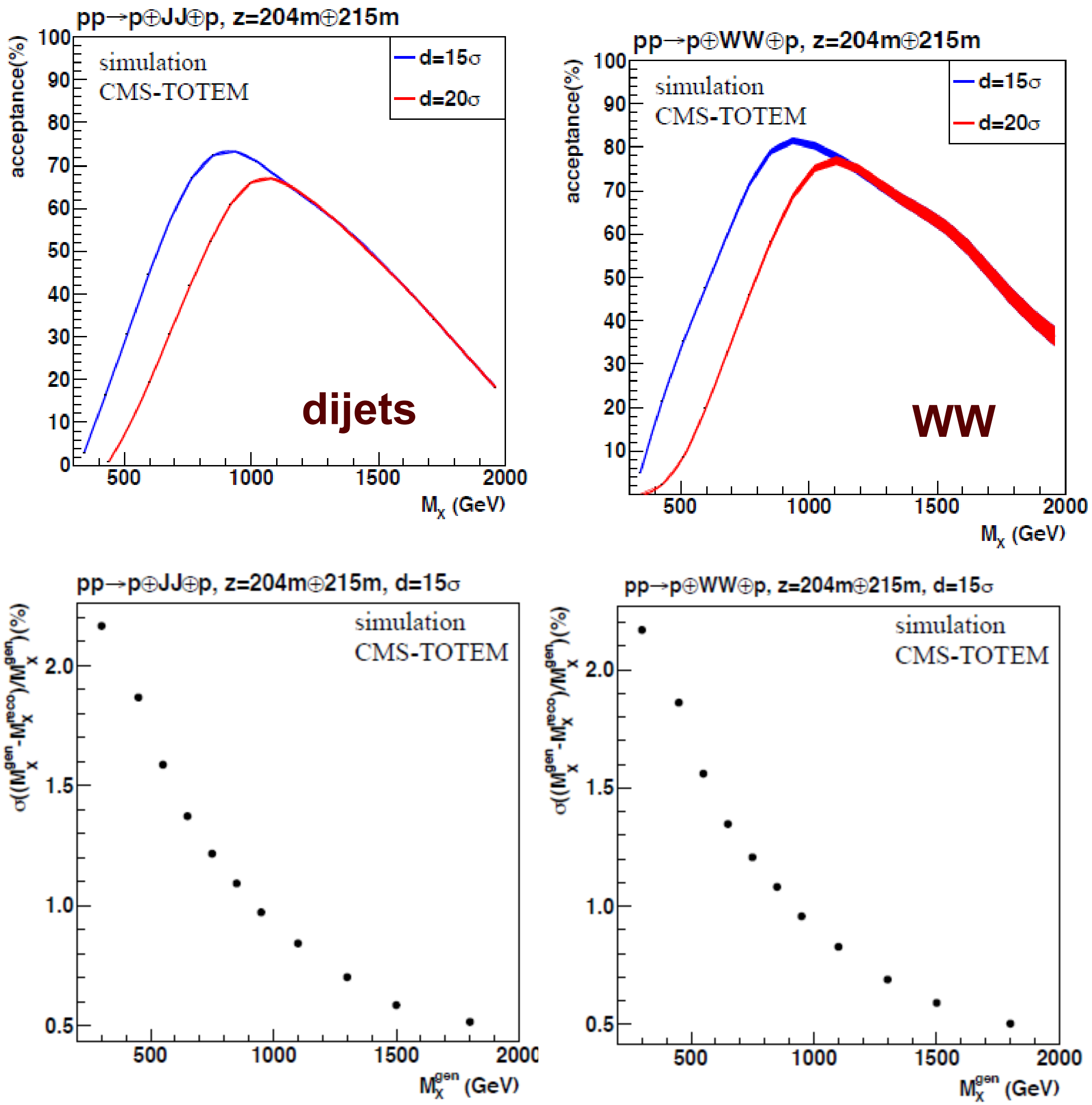

MC simulation: CMS $\gamma\gamma \rightarrow$WW analysis ($\sqrt{s}$=8 TeV)

- **Signal**
  - ✓ SM and anomalous signal samples: MADGRAPH(v2.0.0), based on the equivalent photon approximation (EPA).

- **Backgrounds**
  - ✓ Inclusive WW, ttbar, W+jets processes: MADGRAPH; yields normalized to the NLO cross section predictions obtained with MCFM
  - ✓ Inclusive Drell-Yan process: POWHEG(v1.0)
  - ✓ Exclusive two photon processes: $\gamma\gamma \rightarrow$ll : LPAIR
  - ✓ WW production from single diffractive interactions: POMPYT (v2.6.1); 100% gap survival probability is assumed

  MADGRAPH and POWHEG are matched to parton showers from PYTHIA(v6.4.26) Z2* tune

- **Control samples**
  - ✓ The elastic and proton dissociation $\gamma\gamma \rightarrow l^+l^-$ samples: LPAIR

Systematic uncertainties affecting signal

	Uncertainty
Proton dissociation factor	10.5%
0 extra tracks Efficiency Correction	5.0%
Trigger and lepton ID	2.4%
Luminosity	2.6%
Total	12.1%

Proton dissociation factor:

- 9.2% → statistical uncertainty based on the combination of the $\mu+\mu-$ and e+e– channels.
- 5.0% → difference between the matrix element prediction of LPAIR used for $\gamma\gamma \to l^+l^-$ and the equivalent photon approximation used to generate signal events

Systematic uncertainties considered for the **background** estimation include:

- trigger and lepton ID, luminosity, and simulation statistics
- an uncertainty of ±0.24 events on the electroweak W^+W^- background contribution is included, corresponding to the full difference between the background predictions of the MADGRAPH and PHANTOM generators.

7 TeV data results

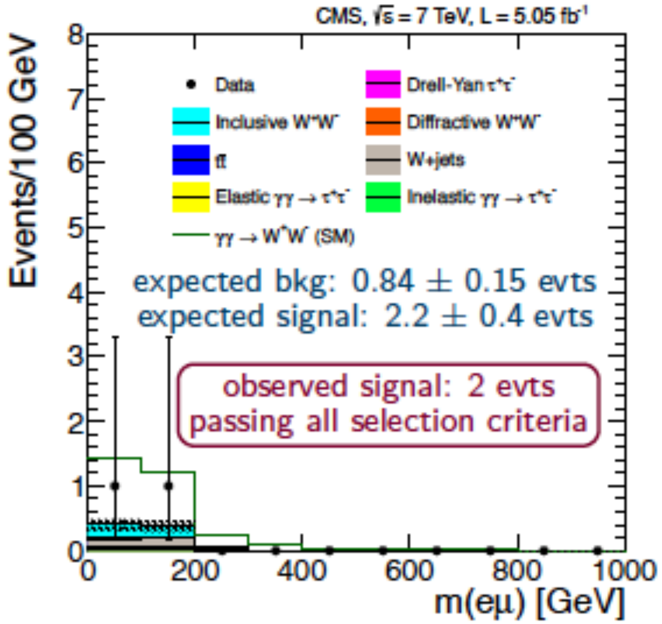

2 events pass all the selection criteria, compared to the expectation of

- 2.2 ± 0.4 signal events
- 0.84 ± 0.15 background events

$$\sigma(pp \to p^{(*)}W^+W^-p^{(*)} \to p^{(*)}\mu^\pm e^\mp p^{(*)}) = 2.2^{+3.3}_{-2.0},$$

Project planning

Exploratory phase (2015-16)

- Prove the ability to operate detectors close to the beamline at high luminosity
  - Show that CT-PPS does not prevent the stable operation of the LHC beams and does not affect significantly the luminosity performance of the machine.
- In 2015:
  - Evaluate RPs in the 204-215 m region
  - Demonstrate the timing performance of the Quartic baseline
  - Use TOTEM silicon strip detectors at sustainable radiation intensity
  - Integrate the CT-PPS detectors into the CMS trigger/DAQ system.
- In 2016:
  - Evaluate the MBP option
  - Upgrade the tracking to pixel detectors
  - Upgrade the timing detectors if required/possible

- **Data Production phase**
  - Aim at accumulating 100 fb^{-1} of data before LHC LS2

Timing detectors for CT-PPS: requirements

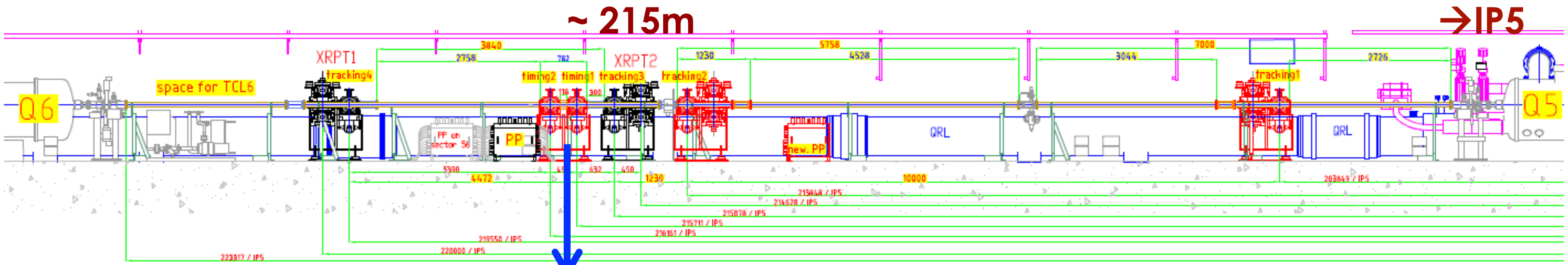

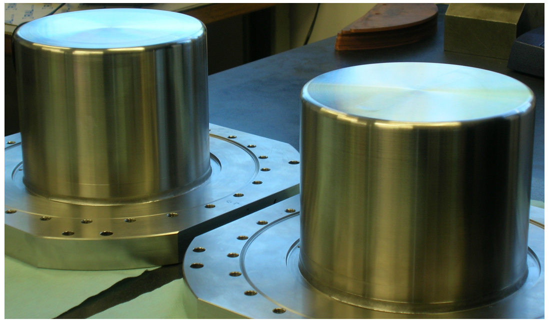

2 new horizontal cylindrical pots

Timing measurement from both sides of CMS allows to determine the vertex of the protons and reject pile-up

- Time resolution ~10 ps →Vertex z-by-timing: ~ 2 mm
- Segmentation to cope with the high occupancy expected
- Edgeless (~ 200 μm)
- Radiation hard

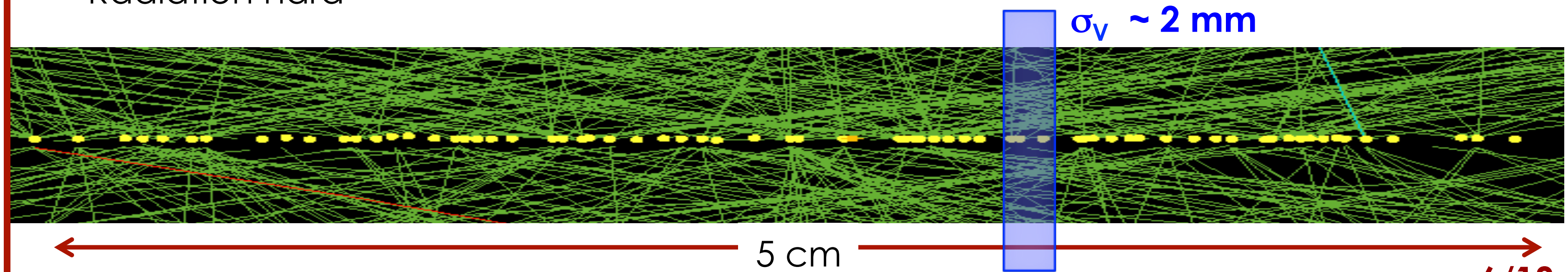

L-bar QUARTIC for PPS

- All Cherenkov light is totally internally reflected along radiator bar

- 66% goes promptly along light guide to SiPM or segmented MCP-PMT.

σ_T ~ 30 ps for 30 mm bar
Four-in-line → 15 ps

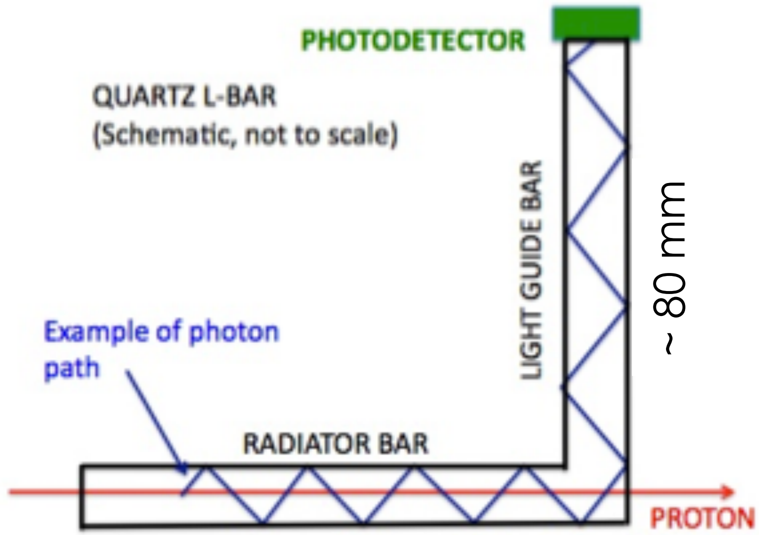

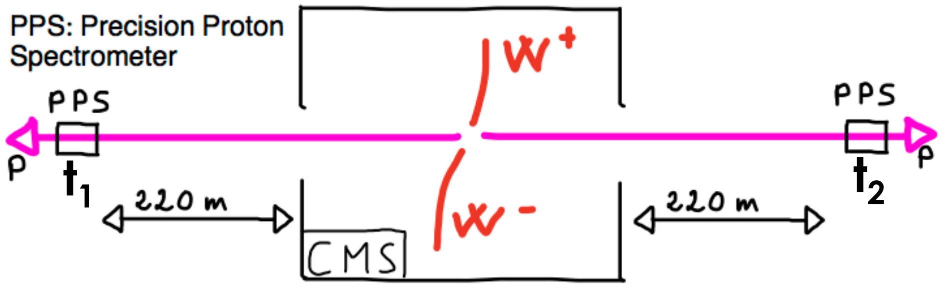

Time difference = $\Delta t = t_1 - t_2$
$z(pp) = 0.5\, c\, \Delta t$
If time resolution $\sigma_T = 10$ps
$\sigma_{\Delta T} = \sqrt{2}\, \sigma_T = 14.1$ ps
$\sigma_Z = 0.5\, c\, 14.1$ ps ~ 2 mm

Timing detectors for CT-PPS: L-bar Quartic

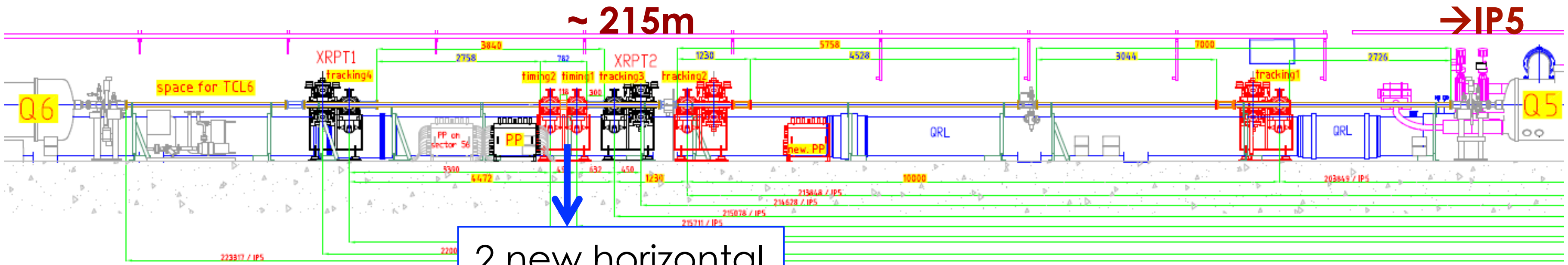

2 new horizontal cylindrical pots

Baseline: L-bar Quartic, Čerenkov detectors with quartz radiators

Module of 3x4 L-bar Quartic

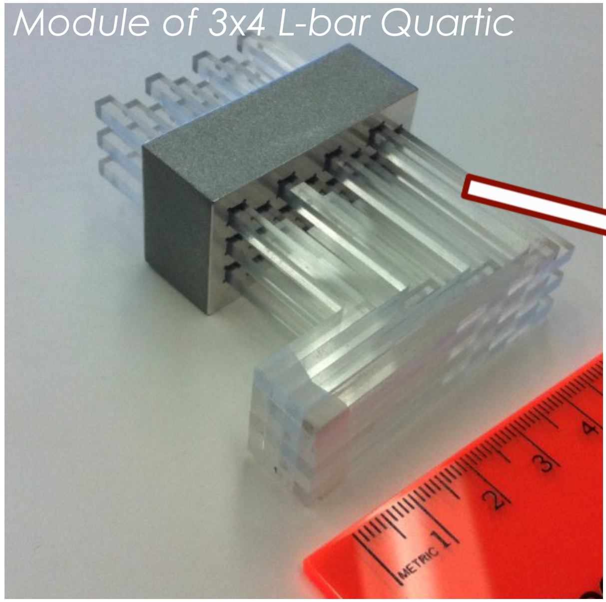

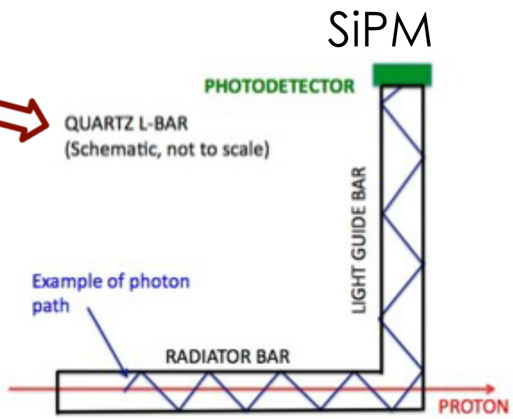

Time resolution measured at test beam

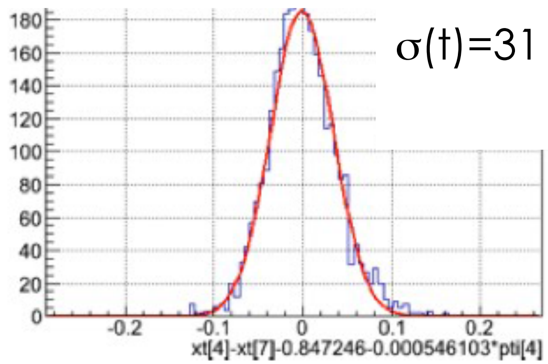

2+2 in-line modules:
$\sigma(t) \sim 15$ ps

Detector installation foreseen at the end 2015

Alternative solutions (for Run2 - post LHC-LS2): diamond, LGAD and 3D

Tracking system for CT-PPS

Two detector stations, ~ 10 meters apart, on each side of IP5

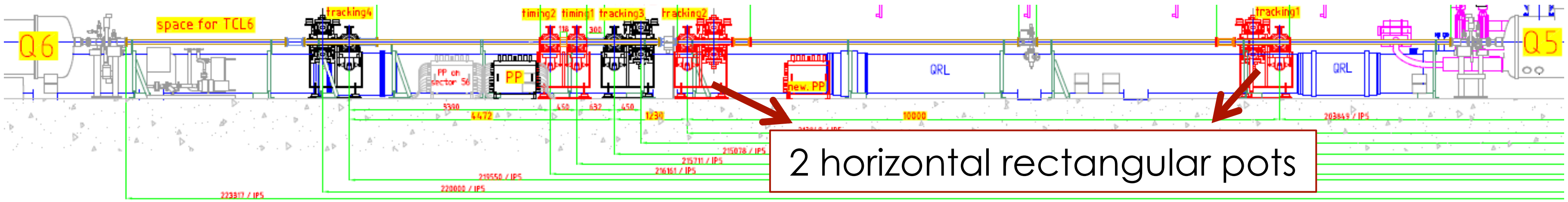

Position and angle, combined with the beam magnets, allow to determine the momentum of the scattered proton and in turn the missing mass:

- Position precision of 10 μm
- Angular resolution of 1-2 μrad

⇨ $\Delta p/p \sim 2\ 10^{-4}$
Mass resolution: ~2 GeV/c^2

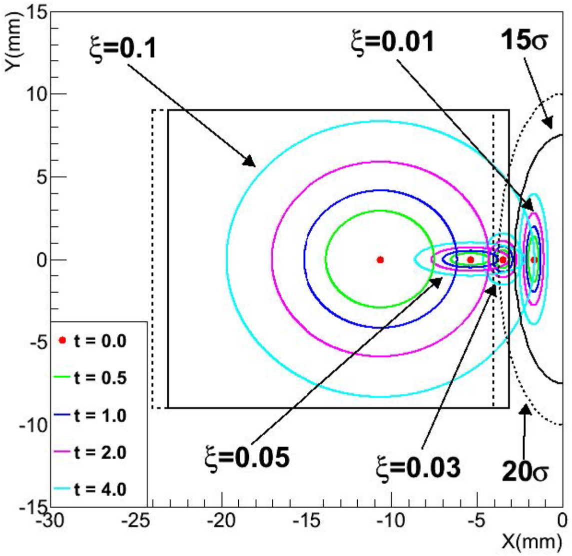

- Slim edges of side facing beam: dead region ~100 μm
- Tolerance to inhomogeneous irradiation: up to $2\ 10^{15}\ n_{eq}/cm^2$ close to the beam (for 100 fb^{-1})
  - Should fit into existing RP

Position of scattered protons at 204 m, for fixed (ξ,t)

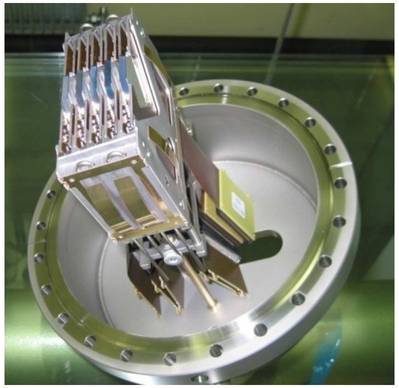

Chosen solution: 3D pixel silicon detectors

Tracking stations

Six detector planes per station

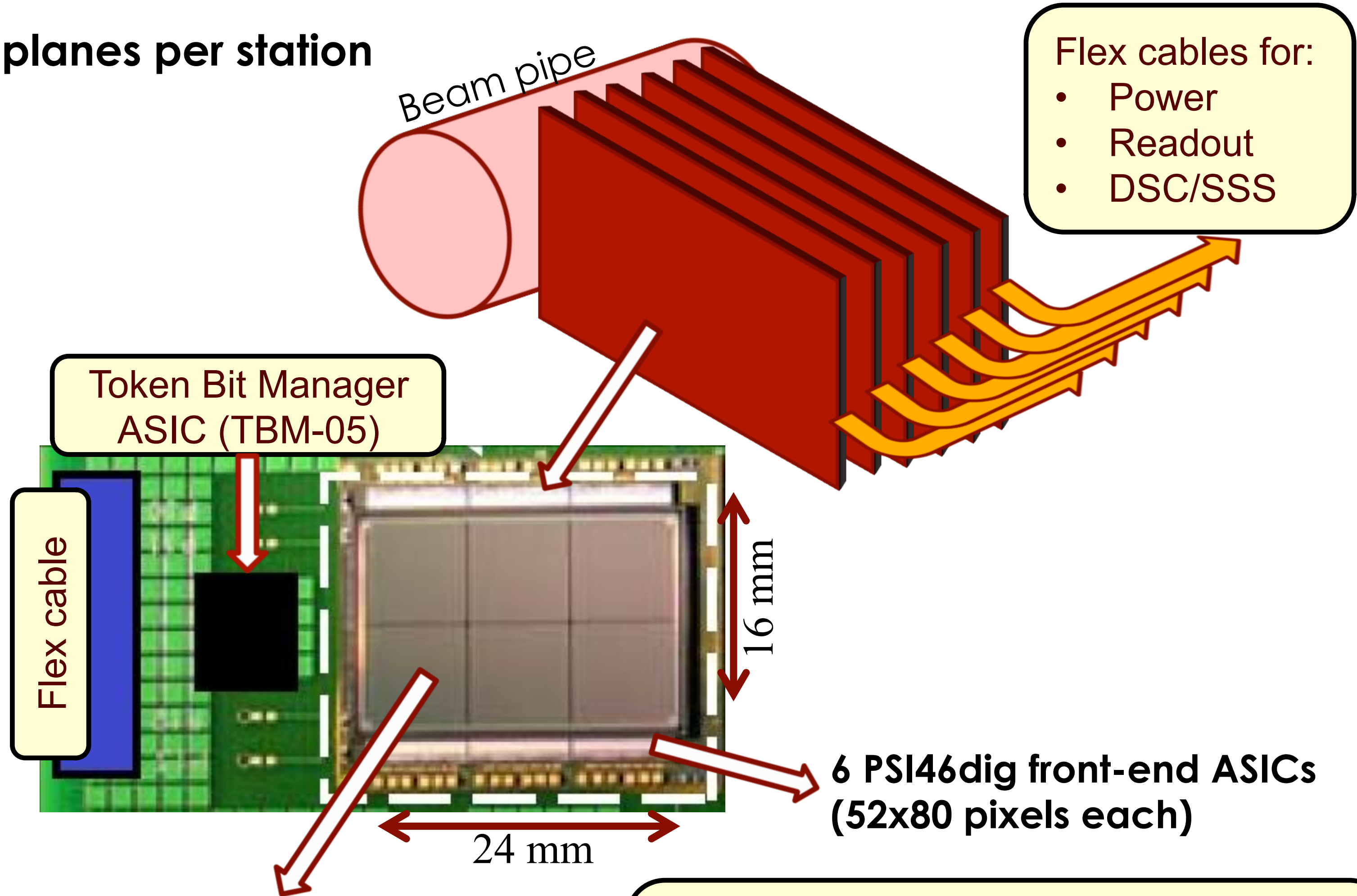

- **16 x 24 mm² 3D pixel silicon sensor**
- **150(y) x 100(x) μm² pixel pattern, same as CMS pixel sensors**

Same readout scheme as Phase-I upgrade of CMS forward pixel system
→ Existing CMS DAQ components and software can be reused

Detector installation foreseen at the end 2016

Why 3D sensors for CT-PPS?

After 15 years of R&D, 3D sensor technology has reached its maturity, as demonstrated by the successful fabrication of more than 300 3D sensors for the ATLAS IBL

3D sensors consist of an array of columnar electrodes [r ~ 5μm] of both doping types that penetrate in the silicon substrate perpendicularly to the surface.

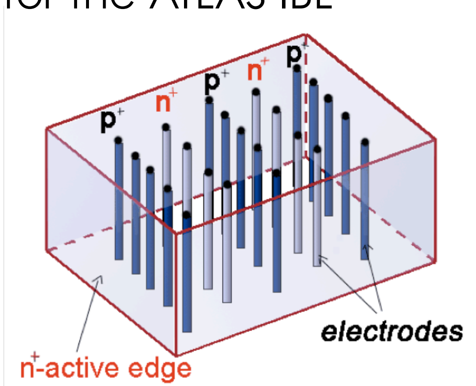

➡ **Electrode distance and active substrate thickness are decoupled**

The close electrode distance provides several advantages w.r.t planar sensor

1. **low full depletion voltage** (~10 V)
2. fast charge collection time
3. reduced charge-trapping probability and therefore **high radiation hardness**.

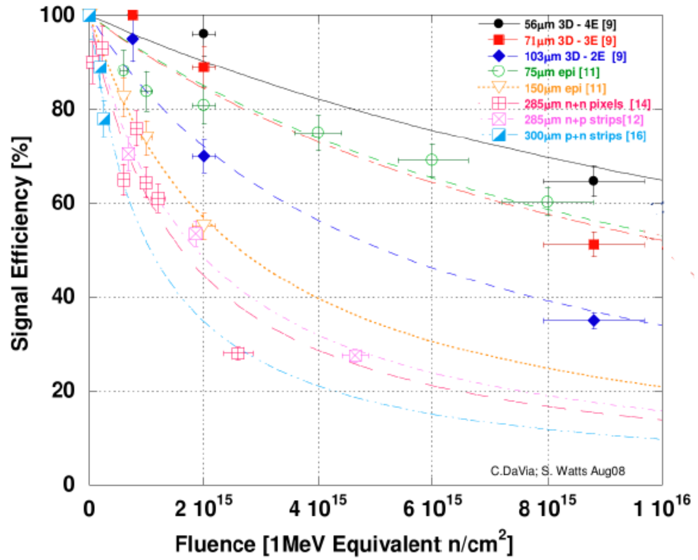

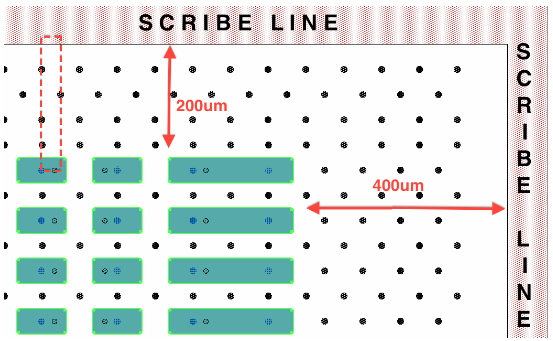

Slim edges, with dead area < 200 μm

Active edges, with dead area reduced to a few μm

Layout details of the corner region of CMS 3D sensors produced by FBK

Roman Pot spectrometer